Available online at www.sciencedirect.com

Coordination Chemistry Reviews 249 (2005) 971–997

COORDINATION CHEMISTRY REVIEWS

www.elsevier.com/locate/ccr

Review

Metallated molecular materials of fluorene derivatives and their analogues

Wai-Yeung Wong*

Department of Chemistry and Centre for Advanced Luminescence Materials, Hong Kong Baptist University,
Waterloo Road, Kowloon Tong, Hong Kong, PR China

Received 23 July 2004; accepted 21 October 2004
Available online 10 December 2004

Contents

Abstract

This review covers recent developments in the molecular design and synthesis of metal-based functional materials of fluorenes and their derivatives. Conjugated organic compounds containing metal centers constitute an important class of molecular materials nowadays because of the combined good features of the chemical, electrochemical, electronic and optical properties of the metal groups to those of the organic chromophores. Recently, substituted fluorene derivatives have been extensively explored in the field of optoelectronics and molecular

---

Abbreviations: bpy, 2,2′-bipyridine; CV, cyclic voltammetry; dafe, 4,5-diazafluorene; dafeN_2, 9-diazo-4,5-diazafluorene; dafo, 4,5-diazafluoren-9-one; DBU, 1,8-diazabicyclo[5.4.0]undec-7-ene; DME, 1,2-dimethoxyethane; DMF, dimethylformamide; DFT, density functional theory; dmit, 1,3-dithiole-2-thione-4,5-dithiolate; DMSO, dimethyl sulfoxide; DP, degree of polymerisation; EFISH, electric-field-induced second-harmonic generation; EPR, electron paramagnetic resonance; FABMS, fast atom bombardment mass spectrometry; Fc, ferrocenyl group ($(\eta^5\text{-}C_5H_5)(\eta^5\text{-}C_5H_4)Fe$); fe, fluorene; fo, fluoren-9-one; GPC, gel permeation chromatography; ICT, intramolecular charge-transfer; IL, intraligand; IR, infrared spectroscopy; ISC, intersystem crossing; ITO, indium-tin-oxide; LB, Langmuir-Blodgett; LED, light-emitting diodes; LF, ligand-field; LLCT, ligand to ligand charge-transfer; MLCT, metal to ligand charge-transfer; NLO, non-linear optics; NMR, nuclear magnetic resonance; OLEDs, organic light-emitting devices; PBD, 2-(4-biphenylyl)-5-(4-*tert*-butylphenyl)-1,3,4-oxadiazole; PEDOT, poly(ethylenedioxythiophene); PEPK, poly[*N*-(2,3-epoxypropyl)carbazole]; phen, 1,10-phenanthroline; PL, photoluminescence; PLEDs, polymer light-emitting devices; PPV, poly(phenylenevinylene); PVK, poly(*N*-vinylcarbazole); SHG, second-harmonic generation; TEM, transmission electron microscopy; terpy, 2,2′:6′,2″-terpyridine; TGA, thermogravimetric analysis; THF, tetrahydrofuran; tren, tris(2-aminoethyl)amine; UV–vis, ultraviolet–visible

* Tel.: +852 34117074; fax: +852 34117348.
E-mail address: rwywong@hkbu.edu.hk.

doi:10.1016/j.ccr.2004.10.007

electronics. They are synthetically easily accessible and possess high thermal and chemical stability as well as high emission quantum yields. Such rapidly emerging chemistry of organic-based fluorene derivatives leads us to believe that a related chemistry involving metal centers should present a fascinating subclass and pose potential for the development of new types of novel materials. While there is great scope for chemical modifications of the metal units and structure of the fluorene ring and its substituents in a systematic fashion, these classes of metal–organics can exhibit rich photophysical, redox and structural properties. An understanding of the structure–property relationships of these molecules allows us to establish good model systems in the development of optoelectronic devices, molecular electronics and chemical sensing applications. In this article, homo- and heterometallic systems containing fluorene chromophores and their structural analogues such as carbazoles and diazafluorenes are discussed, and particular attention is paid to chemical reactivities, electronic absorption spectroscopy, photoluminescence and redox behavior, and structural aspects of these metal–organic compounds. The applications that these materials have found in various domains are also highlighted.

Keywords: Conjugated molecules; Carbazoles; Diazafluorenes; Fluorenes; Metal complexes

1. Introduction

The past few decades have witnessed an explosion in the field of organic-based conjugated materials [1–7]. Since the first demonstration of polymer light-emitting diodes (PLEDs) using the poly(phenylenevinylene) (PPV) in 1990s [8], work on conjugated polymer materials has intensified and numerous conjugated organic polymers have been extensively explored in this aspect. Conjugated polymers with different chemical structures emitting different colors in the whole visible range have been designed and devices based on these materials have been fabricated [8–11]. Although many challenges remain before this area can be fully commercialized, it is conceived that the next generation of flat screen displays could be fabricated from these PLEDs and the emission colors can be systematically tuned by variation of the chemical structures of the molecules concerned.

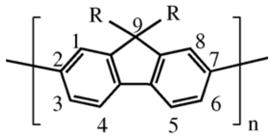

Fig. 1. Chemical structure of poly(2,7-fluorene) derivatives.

Despite the plenty of fruitful results acquired in a vast body of work on organic-based materials, recently, there are strong motivations for synthetic chemists to incorporate metal units into organic and polymer structures [12–17]. The key interest in this research area is to determine the nature and extent of the electronic coupling between the metal and conjugated backbone units, therefore, much attention has been focused on building and studying model complexes in which metal groups are tethered to conjugated fragments via different linkages, and examining the nature of the coupling in these systems. Several excellent reviews and books are available in relation to these synthetic metal-containing compounds [12–17]. While electronic interactions in some metallated polythiophenes have been reviewed recently by Stott and Wolf [18], the related chemistry of polyfluorenes is still in its infancy and is worthy of attention. The major focus of this review is to survey the metal complexes of fluorene deriva-

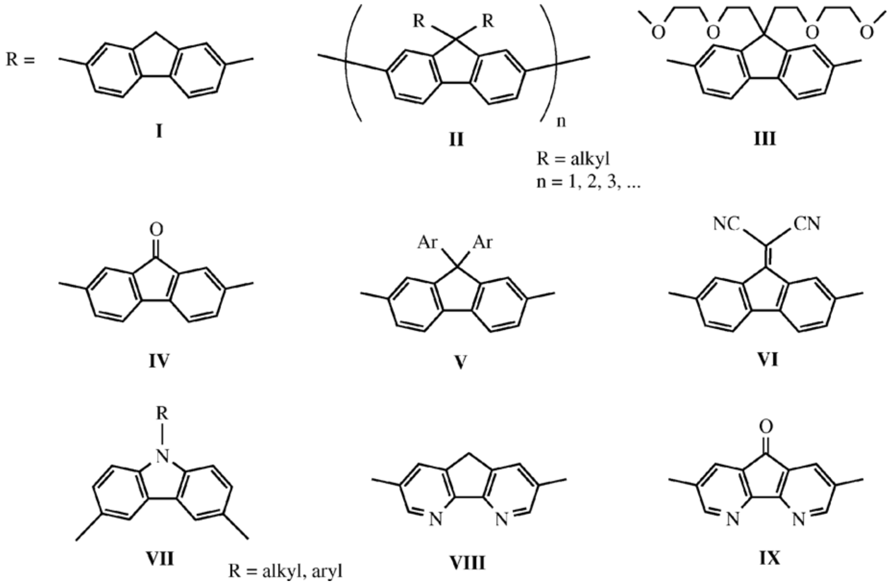

Fig. 2. Structures of substituted fluorene derivatives and their analogues.

tives in the literature and to investigate the importance of these metallated compounds in the field of materials science.

2. Oligo- and polyfluorenes

Fluorene, in organic polymers, provides a significant contribution to the field of electronic materials [19,20]. The use of fluorenyl chromophores and other related derivatives such as carbazoles offers exciting perspectives for the design of new molecular and polymeric materials for various optoelectronic applications. The ease of modification and knowledge of the structure–property relationships of polyfluorene homopolymers and copolymers continue to make the fluorene-functionalized compounds very attractive candidates in the development of new functional materials. It is well-known that substituted poly(2,7-fluorene) derivatives (Fig. 1) are attractive as active components of organic light-emitting diodes (OLEDs) due to their thermal and chemical stability and their high emission quantum yields [21–23]. The fluorene structural moiety provides a rigidly planar biphenyl unit within the molecular backbone. Substituent derivatization at the C-9 position of the monomeric fluorenes provides the prospect of controlling polymer properties such as solubility, emission wavelengths, processability and mediating potential interchain interactions in films [24–29]. In this regard, a number of elegant synthetic routes have been developed to generate fluorene-containing materials. Moreover, substituted fluorenes are widely used as electron acceptors in charge transfer complexes with semiconducting and photoconducting properties and as electron transport materials [30,31]. Fluorene acceptors are also known for their ability to sensitize the photoconductivity of poly(*N*-vinylcarbazole) (PVK) and other related polymers [32–34]. Fig. 2 lists some common building blocks known in the literature for this purpose; they encompass fluorene (**I**–**VI**), carbazole (**VII**) and diazafluorene (**VIII** and **IX**) chromophores.

3. Metallated complexes of fluorenes and their derivatives

Initially, most of the conjugated systems were based on purely organic backbones, but subsequently there has been a tremendous push around the world to incorporate metal complexes into electronically extended frameworks [12–18]. The presence of metal centers has been shown to give rise to a diverse range of interesting and often useful redox, magnetic, optical, electrical, and catalytic properties. These features provide a key motivation for making these metal-based materials. This line of research also plays a pivotal role in determining the nature and extent of the electronic coupling between the metal and conjugated backbone units. This review is intended to provide a comprehensive account of metal complexes of fluorenes and their analogues, all of which can exhibit rich photophysical, redox and structural properties.

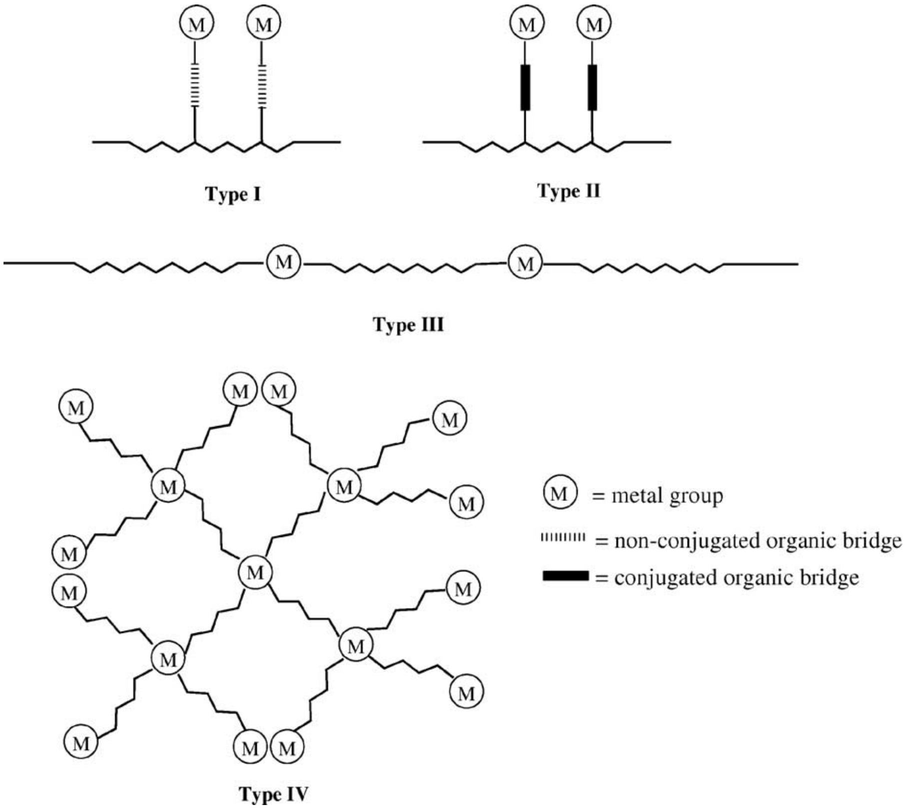

Fig. 3. Structural types of metal-containing conjugated molecules.

In the literature, several possible metal-containing structural skeletons exist, depending on where the metal atoms are incorporated and the nature of the linking units between them (Fig. 3). The metals can either be in the side-group structure (types I and II) or directly in the main chain (type III). The key difference between types I and II is that the former contains isolated pendant metal functionalities whilst the latter carries electronically coupled metal groups. Dendrimers and hyperbranched structures (type IV) represent another structural class of growing interest. In this case, the metallo-centers can be located throughout the structure or, alternatively, in the core or at the periphery. In the following discussion, we will focus on some recent advances in the synthesis and chemistry of a wide range of metallated complexes of fluorene derivatives, grouped according to the nature of the organic spacers.

3.1. Fluorene groups

3.1.1. C-donors

The design and synthesis of metal σ-alkynyl complexes and polymers with unusual optoelectronic properties has aroused the interest of many research groups [35–37]. These complexes hold a fascination for synthetic chemists, structural chemists and materials scientists alike. The linear geometry of the alkynyl moiety and its unsaturated backbone make the organometallic alkynyls attractive and versatile building units for molecular wires and organometallic oligomers and polymers which can lead to unique features such as luminescence, liquid crystallinity, optical non-linearity and electrical and photoconductivity.

New bis(ferrocenylethynyl) complexes with fluorenyl-based spacers **1**–**3** were prepared in good yield by Sonogashira coupling reactions of ethynylferrocene with the corresponding dibromofluorene derivatives in a 2:1 molar ratio [38]. The crystal structures of **1** and **2** were determined. Although cyclic voltammetry (CV) shows that the two ferrocenyl end groups only weakly communicate through the fluorenyl ring system, the half-wave potentials of the terminal ferrocenyl units show a gradual increase in the order **3** < **2** < **1** upon changing the substituent at the 9 position of the fluorenyl ring from the electron-donating ferrocenyl group in **3** to an electron-withdrawing oxo group in **1**. The potential is shifted positive by ca. 110 mV from **3** to **1** and the low oxidation potential value in **3** shows that such a triferrocenyl species is electron-rich. Loss of electron density from the ferrocenyl donor unit to the net electron-accepting fluorenone moiety through the alkynyl linking unit makes the oxidation wave appear at a more positive potential in **1**.

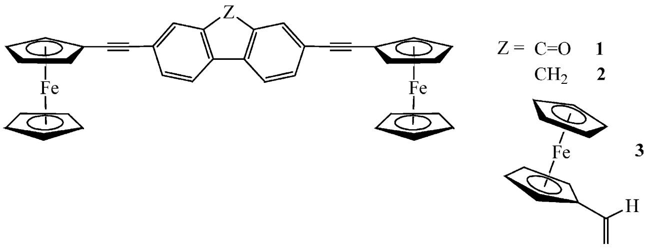

Z = C=O **1**
CH$_2$ **2**
3

Starting from the precursors 2-ethynyl-7-(2-ferrocenylethynyl)fluoren-9-one and 2-ethynyl-7-(4-ferrocenylphenylethynyl)fluoren-9-one, a series of ferrocenyl heterometallic systems of 2,7-diethynylfluoren-9-one **4**–**11** have been prepared and well characterized [39,40]. The redox chemistry of these mixed-metal compounds were investigated by CV. It was found that oxidation of the ferrocenyl moiety is facilitated by the presence of the metal center and increased conjugation in the chain through the ethynyl and fluorenone linkages. The crystal structures of **4**, **6**–**9** and **11** were also established. For **6** and **7**, there is a centrosymmetry at the plat-

Fig. 4. Space-filling model of **6**.

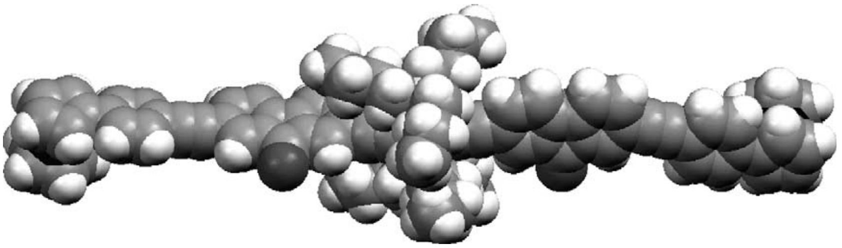

Fig. 5. Space-filling model of **7**.

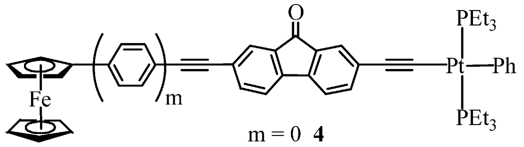

m = 0 **4**
m = 1 **5**

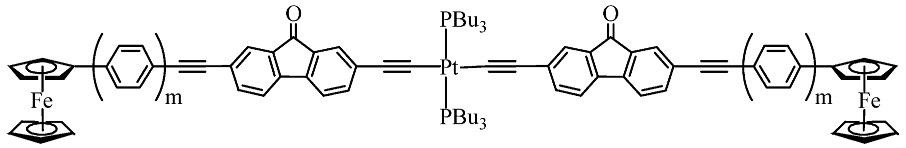

m = 0 **6**
m = 1 **7**

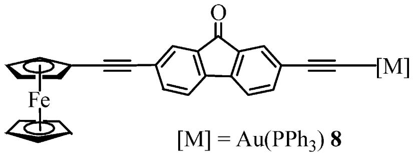

[M] = Au(PPh_3) **8**
[M] = MeHg **9**

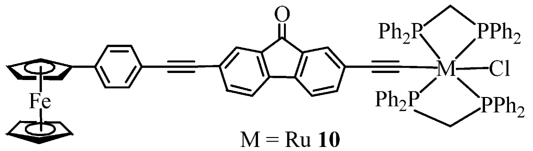

M = Ru **10**
M = Os **11**

inum center in each case to give a one-dimensional molecular rod of defined length. Iron–iron through-space separation distances of ca. 34 and 42 Å are observed, respectively (Figs. 4 and 5). In this way, extension of the dimensions of these rigid-rod metal-capped molecules from molecular scale to nanoscale becomes viable. The electronic absorption data of these molecules were correlated with theoretical results obtained by density functional theory (DFT). Introduction of the platinum(II) segment in **6** and **7** red-shifts the lowest energy bands and increases the absorption intensity, suggesting an enhancement in the extent of π-delocalization through the platinum conjugated system.

Unexpectedly, the coupling reaction of 2,7-dibromo-9-(dicyanomethylene)flurorene with ethynylferrocene afforded an unsymmetrical mono-cyano substituted fluorene compound **12** in which one of the cyano groups is substituted by the incoming ferrocenylacetylide moiety (Scheme 1) [41]. This contrasts with the classical palladium-catalyzed Sonogashira coupling of aryl halides with terminal acetylenes for the introduction of an ethynyl group into organic structures [42]. This reaction was also shown to work very well for organic terminal acetylenes. To make the symmetrical product **13**, the fluoren-9-one derivative **1** was condensed with malononitrile. The crystal structure of **12** was determined and it represents the first structurally characterized example of a fluorene derivative possessing an σ-acetylide group at its 9-methylene position. The electronic spectra of **12** and **13** are characterized by the structureless $\pi \rightarrow \pi^*$ transition bands of the corresponding fluorene π skeleton as well as metal to ligand charge-transfer (MLCT) transitions at the low-energy regime. These assignments were supported by molecular orbital calculations. We note a bathochromic shift of ca. 0.52 eV in λ_{max} in going from **1** to **13**. The observation of solvatochromic phenomenon for the lowest energy MLCT band in **12** (a red-shift of 0.11 eV from hexane to CH_2Cl_2) is consistent with a dipolar excited state due to intramolecular charge-transfer (ICT) transition from the electron-donating ferrocenyl group to the electron-withdrawing cyano group

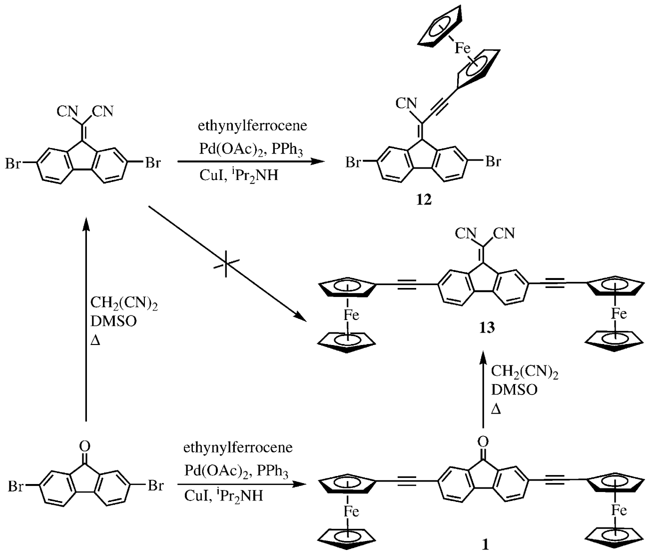

Scheme 1.

through the conjugated system. Analogous electron donor-π-acceptor chromophores **14a** and **b** were also reported by Perepichka and co-workers which were obtained from the reaction between formylated ferrocenylacetylene and substituted fluorenes [43]. Compounds **14a** and **b** show ICT bands from the donor onto the acceptor moiety at 1.88 and 2.01 eV, respectively, and moderate second-order NLO properties as determined by the EFISH technique at $\lambda = 1.54\,\mu$m were observed for **14b** [$\mu\beta(0) \approx 170 \pm 30 \times 10^{-48}$ esu]. The authors have also demonstrated in these cases that the polynitrofluorene moiety is a much better terminal acceptor group in NLO chromophores than the dicyanomethylene moiety.

By reaction of ferrocenecarbaldehyde, its vinylogue, and ferrocene or ruthenocene dicarbaldehydes with substituted nitrofluorenes, four classes of metallocene-fluorene push–pull complexes **15–19** were synthesized and spectroscopically characterized [44]. CV studies indicate reversible formation of ferrocenium cation and reversible stepwise single-electron reductions to radical anion and dianion species which merge into one two-electron reduction process with decreasing electron acceptor ability of the fluorene group. The push–pull nature of these compounds were found to result in ICT bands metallocene to acceptor fluorene fragment, which was probed by electronic absorption studies. Due to the strong ICT in complexes **15a–g**, which can be represented by zwitterionic resonance structures, the rotation barrier around the formally CH=fluorene exocyclic double bond is expected to be relatively low and hence *E*–*Z* isomerization can occur in solution to afford mixtures of *E* and *Z* isomers (as confirmed by ^{1}H NMR spectroscopy). Elongation of the π-bridge (from one π-orbital in **15** to five π-orbitals in **19**) tends to red-shift the ICT band by 0.13–0.24 eV and increase the absorption intensities. Substitution of Fe in compounds **17a–c** by Ru in **18a–c** results in a hypsochromic shift (ca. 0.38–0.43 eV) of ICT because of the lowered donor ability of the metallocene unit. Energies of ICT and reduction potentials were shown to display excellent correlation with Hammett-type substituents constants in the fluorene structure. Compounds **15–19** display solvatochromism in solvents of different polarity. Acceptor **15a** was demonstrated to sensitize the photoconductivity of poly[*N*-(2,3-epoxypropyl)carbazole] (PEPK) showing moderate holographic response of the materials. Determination of crystal structures for **15a**, **15g** and **16a** revealed π–π stacking of fluorene rings in the latter two cases but steric effects between nitro groups in positions 4 and 5 of **15a** prevent π–π stack formation.

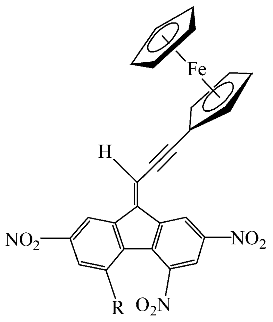

R = NO_2 **14a**
R = $CO_2(CH_2CH_2O)_3Me$ **14b**

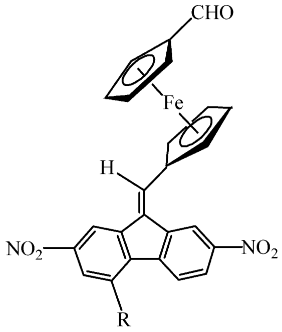

R = NO_2 **16a**
R = CN **16b**

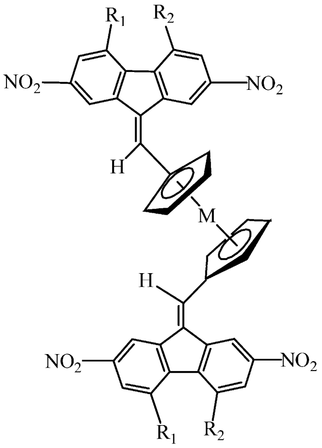

M = Fe
$R_1 = R_2 = NO_2$ **17a**
$R_1 = NO_2$, R_2 = CN **17b**
$R_1 = NO_2$, $R_2 = CO_2Me$ **17c**

M = Ru
$R_1 = R_2 = NO_2$ **18a**
$R_1 = NO_2$, R_2 = CN **18b**
$R_1 = NO_2$, $R_2 = CO_2Me$ **18c**

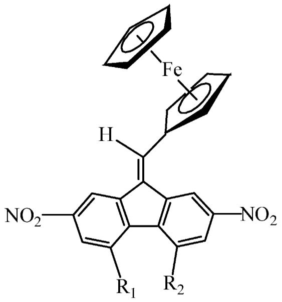

$R_1 = R_2 = NO_2$ **15a**
$R_1 = NO_2$, R_2 = CN **15b**
$R_1 = NO_2$, $R_2 = CO_2Me$ **15c**
$R_1 = NO_2$, R_2 = H **15d**
R_1 = CN, R_2 = H **15e**
$R_1 = CO_2Me$, R_2 = H **15f**
$R_1 = R_2$ = H **15g**

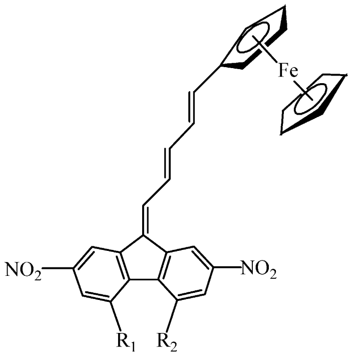

$R_1 = R_2 = NO_2$ **19a**
$R_1 = NO_2$, R_2 = CN **19b**
$R_1 = NO_2$, $R_2 = CO_2Me$ **19c**
$R_1 = NO_2$, R_2 = H **19d**
R_1 = CN, R_2 = H **19e**

Homometallic diyne complexes **20** and **21** and a mixed metal diyne complex of ruthenium and osmium **22** were synthesized via the $NaPF_6$/DBU method through the formation of the vinylidene intermediates [45]. In the cyclic voltammogram, the heterobimetallic Ru^{II}/Os^{II} complex **22** displays two well-separated ($\Delta E_{1/2} = 0.24$ V) quasi-reversible oxidation processes centered at −0.31 and −0.07 V, attributed to the two one-electron oxidations at the osmium and ruthenium centers, respectively. From the CV of **22**, it may be concluded that the ruthenium center releases electron density to the osmium unit via the central diethynylfluorenonyl bridge and thus the electrode potential of the Os^{III}/Os^{II} couple is lowered significantly from −0.20 to −0.31 V. Electrochemical investigations of the homometallic dimeric complexes **20** and **21** showed a similar trend and they show two successive, closely spaced quasi-reversible oxidation waves which could be ascribed to the formation of the mono- and dications, respectively, corresponding to the M^{III}/M^{II} and M^{III}/M^{III} (M = Ru, Os) couples. The redox processes can be interpreted as:

$$\mathrm{Os^{II}/Ru^{II}} \xrightleftharpoons[+e]{-e} \mathrm{Os^{III}/Ru^{II}} \xrightleftharpoons[+e]{-e} \mathrm{Os^{III}/Ru^{III}}$$

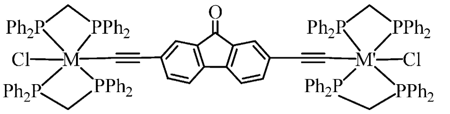

M = M' = Ru **20**
M = M' = Os **21**
M = Ru, M' = Os **22**

The synthesis and electrochemistry of a series of organometallic dimers of the form $[\{Co_2(CO)_6\}_2(\text{diyne})]$ **23**–**28** were reported [46]. The solid-state structures of four of them are known. Low-temperature CV experiments show that the two $Co_2(CO)_6$ redox centers are electronically coupled and the extent of interactions can be modulated by the donor–acceptor characteristics of the central spacer. The splitting between the two well-resolved reversible couples is largest in the presence of an electron-donating ferrocenyl group and the smallest peak separation is achieved with an electron-withdrawing fluorenone moiety.

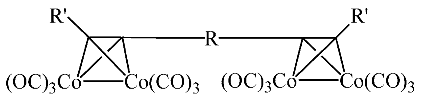

R = 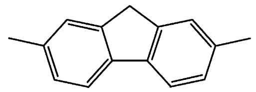 R' = Me3Si **23** ; R' = H **26**

R = 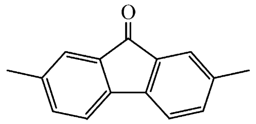 R' = Me3Si **24** ; R' = H **27**

R = 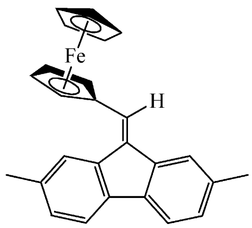 R' = Me3Si **25** ; R' = H **28**

Table 1
Optical data of various platinum(II) fluorene-based materials

Compound where Z=	Color	Lowest energy band in CH_2Cl_2 (eV)	E_g (eV)	Reference
CH_2	Off-white	3.15	2.90	[47]
$C(C_6H_{13})_2$	Off-white	3.11	2.92	[49]
C=O	Red	2.45	2.10	[45]
C=C(H)Fc	Red	2.84	2.10	[47]
$C{=}C(CN)_2$	Blue	1.88	1.58	[48]
$N(C_4H_9)$	Off-white	3.60	3.10	[49]

Recently, the chemistry and photophysics of new platinum(II) diynes and polyynes containing fluorene auxiliaries were extensively explored [47–50]. The strong spin–orbit coupling associated with these heavy metals enables significant mixing of singlet and triplet states, which renders the spin-forbidden emission from the triplet excited state (i.e., phosphorescence or triplet emission) partially allowed and experimentally more accessible using optical spectroscopy, which is often not the case for hydrocarbon conjugated polymers. Monomeric (**29**–**34**) and polymeric complexes (**35**–**40**) of platinum(II) were prepared by the dehydrohalogenation procedures using the CuI/$^iPr_2NH$ catalytic system. All these platinum complexes readily dissolve in aprotic solvents and exhibit good thermal stability. The polymers are easily processable from organic solvents and exhibit good film-forming properties. The three-dimensional solid-state structures of **29**, **33** and **34** were confirmed by single-crystal X-ray analyses. Generally, model diyne monomers can be considered as building blocks for the high molecular weight polymers and valuable information concerning their molecular and electronic properties can be obtained through the studies of these model compounds.

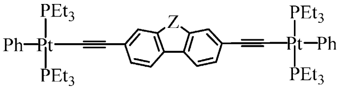

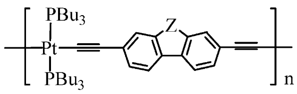

	Monomers	Polymers
Z = CH_2	**29**	**35**
$C(C_6H_{13})_2$	**30**	**36**
$C(C_8H_{17})_2$	**31**	**37**
C=O	**32**	**38**
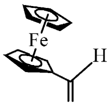	**33**	**39**
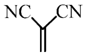	**34**	**40**

By varying the substituents at C-9 position of fluorene ring, the optical absorption and emission properties of these metal-containing polymers can be chemically tuned. These platinum(II) compounds exhibit a variety of colors and optical gaps in the solid states (Table 1). The dependence of the first excited singlet and triplet electronic state on the chemical structure of the fluorene spacer groups of these systems was systematically investigated. It was found that the position of the lowest energy absorption band is red-shifted when the platinum group is introduced. This reveals that π-conjugation of the ligands extends through the metal center. The transition energies of the polymers are lowered with respect to those of the corresponding monomers. The bandgap of **40** is estimated to be 1.58 eV which is currently the lowest reported for metal polyyne polymers. A systematic correlation was made between the effective conjugation length (or conversely, optical gap, E_g) and the intersystem crossing (ISC) rate in these polyynes. The larger the bandgap, the higher the efficiency of triplet emission.

Raithby and co-workers also recently compared the photophysical properties of several platinum(II) polyynes **35**, **37** and **38** with their organic co-polyynes [50]. Since the non-radiative decay rate from the T_1 triplet state is equal or larger than the radiative decay rate, the photoluminescence (PL) quantum efficiencies of the platinum polyynes are reduced from those for the organic polymers. Optical spectroscopic measurements reveal that the attachment of octyl side chains on the fluorenyl spacer reduces interchain interaction in the polyynes while a fluorenonyl spacer creates a donor–acceptor interaction along the rigid backbone. Conjugated copolymer **41** possessing a pendant ferrocene moiety is also known and its spectroscopic, redox and thermal behavior have been investigated [51,52].

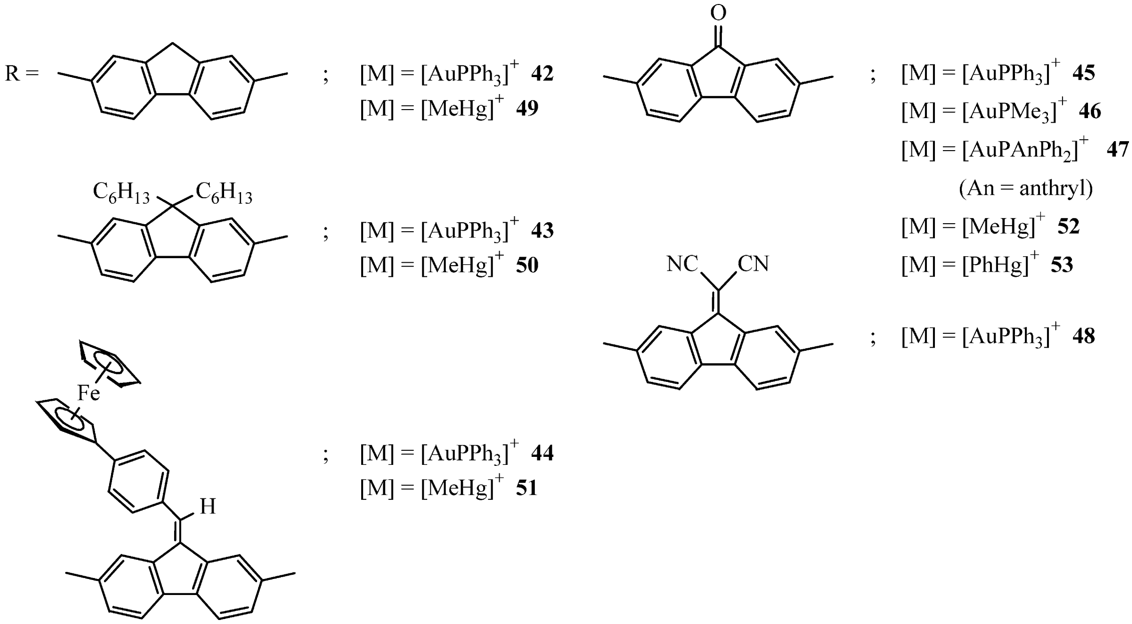

; [M] = $[AuPPh_3]^+$ **42**
[M] = $[MeHg]^+$ **49**

; [M] = $[AuPPh_3]^+$ **43**
[M] = $[MeHg]^+$ **50**

; [M] = $[AuPPh_3]^+$ **44**
[M] = $[MeHg]^+$ **51**

; [M] = $[AuPPh_3]^+$ **45**
[M] = $[AuPMe_3]^+$ **46**
[M] = $[AuPAnPh_2]^+$ **47**
(An = anthryl)
[M] = $[MeHg]^+$ **52**
[M] = $[PhHg]^+$ **53**

; [M] = $[AuPPh_3]^+$ **48**

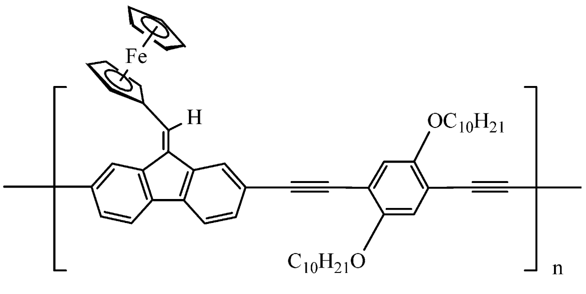

41

Single-layer photocells of the type ITO/polymer/Al (ITO = indium-tin-oxide) were fabricated for **36** and **40**. Both of them exhibit moderate photoconductivity and they show a photocurrent quantum yield of approximately 0.01%, which is a common value for single-layer devices. The authors found that there is no significant difference in the quantum efficiency with variation of the central fluorene ring [49].

The first synthesis and spectroscopic characterization of a series of novel bis(alkynyl) gold(I) and mercury(II) complexes **42**–**53** with electron-rich and electron-deficient fluorene moieties were accomplished recently [53]. The product yields of these compounds were very high (>80%). Complexes **43**, **45** and **52** were characterized by X-ray crystallography and the crystal structure of **52** represents the first structurally characterized example of a dimercury(II) diacetylide (Fig. 6). Their electronic, luminescent and redox behavior was investigated as a function of the metal groups and their auxiliary ligand groups as well as the peripheral substituents of the central fluorene ring.

The first examples of soluble well-defined high molecular weight mercury(II) polyyne polymers with 9,9-dialkylfluorenes were reported by our group [54]. Estimates of the molecular weights using GPC in THF indicate a high degree of polymerization (DP = 24–47) in these polyynes. Starting with 2,7-diethynylfluorene, only an intractable solid was obtained and thus it is critical to use long alkyl side chains to ensure high solubility of the polymers. Polymers **54**–**56** displayed moderate thermal stability. Polymer **56** shows the lowest onset decomposition temperature, while **54** and **55** with shorter alkyl chains exhibit increasing decomposition temperatures with decreasing *m* value. The presence of the heavy group 12 mercury(II) center should enhance spin–orbit coupling and it was shown for the first time that the organic triplet emissions of fluorenyleneethynylenes have been “illuminated” by the heavy-atom effect of mercury. Complex **57**, a model complex of **55**, was also synthesized, in which one

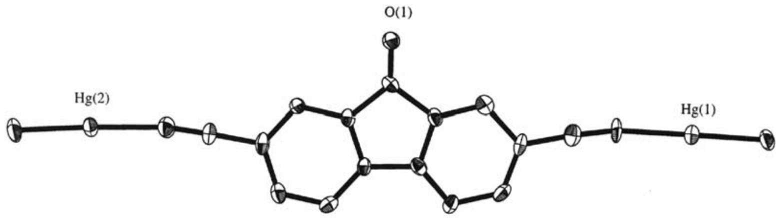

Fig. 6. X-ray structure of **52**.

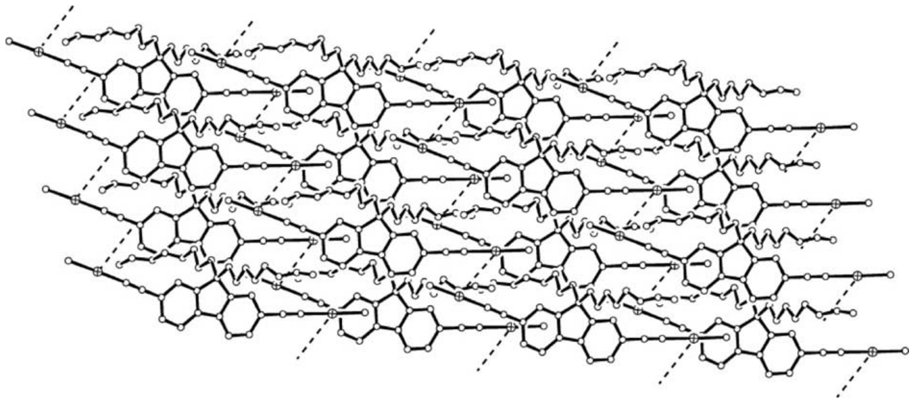

Fig. 7. Crystal packing diagram for **57**. The weak intermolecular mercuriophilic contacts in a 3D network are represented by the dashed lines.

coordination site is protected by a Me group. The X-ray structure of **57** also helped to establish polymer structures in the solid state and to correlate the photophysical properties with the structural data. It consists of dinuclear molecules in which the mercury centers adopt a two-coordinate linear geometry in a rigid-rod manner. The lattice structure is highlighted by the presence of weak intermolecular noncovalent Hg···Hg interactions (3.738 and 4.183 Å), which link the molecular units together to form a loose polymeric structure in a 3D network (Fig. 7). The Hg···Hg interaction distances in **57** are towards the upper limit of those accepted as representing metallophilic interactions [55–58].

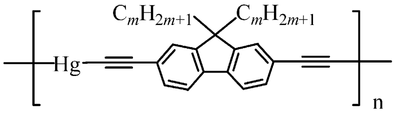

$m = 6$ **54**
$m = 8$ **55**
$m = 16$ **56**

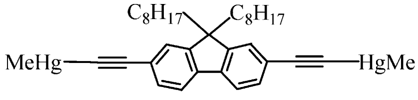

57

The photophysics of **54**–**57** were examined. A red-shift of absorption and emission bands in **54**–**57** was noted after the inclusion of a heavy metal atom, which indicates an increase in π-conjugation. The transition energies of **55** are lowered with respect to those of the monomer **57**, suggesting a well-extended singlet excited state in the polymers. Examination of the absorption behavior of the polymers in $CHCl_3$, $CHCl_3$/MeOH solutions, and in the solid state, corroborates the presence of solid-state aggregates in thin films [59] which also agrees well with the solid-state mercuriophilic interactions in the crystal structure of **57**. At 11 K, lower-lying phosphorescent emissions emerge around 570–590 nm for **54**–**56**. The order of S_1–T_1 crossover efficiency is **56** > **55** > **54**. The ISC rate is also higher in the polymers than in the monomers. Considering the spatial extent of the singlet and triplet excitons in such a system, values of $\Delta E(S_0–T_1)$ (energy gap between S_0 and T_1) were found to be 2.10–2.23 eV for **54**–**56**. The $\Delta E(S_1–T_1)$ values for **54**–**56** lie within the range of 0.73–0.79 eV and they match well the S_1–T_1 energy gap of 0.7 ± 0.1 eV for similar π-conjugated Pt(II) and Au(I) polyynes [60–66].

Recently, the synthesis and luminescent properties of a new series of metal diynes **58** and polyynes **59** of group 10–12 transition metals containing the conjugation-interrupting diphenylfluorene unit appeared in the literature [67]. All three metals (viz. Pt, Au and Hg) can exert heavy-atom effects in the enhancement of ISC rate, and the effect is most significant for Pt having the highest T_1 energy state. The sp^3-carbon site in diphenylfluroene is an effective conjugation-interrupter to limit the conjugation length in metal polyynes, leading to materials with high optical gaps and high-energy triplet states.

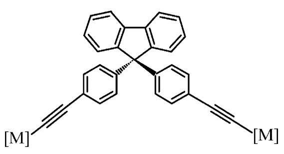

[M] = PhPt$(PEt_3)_2$, Au(PPh_3), MeHg

58

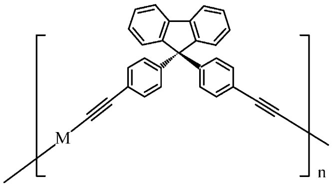

[M] = Pt$(PBu_3)_2$, Hg

59

The interactions of 9-ethynylfluoren-9-ol with some bimetallic and multimetallic systems were examined. The thermal reaction of $[Ru_3(CO)_{12}]$ with 9-ethynylfluoren-9-ol in THF gave five new ruthenium fluorene clusters **60**–**64** in low yields which were fully characterized by IR, NMR, FABMS and X-ray crystallographic studies [68]. Most of them exhibited interesting structural features. The synthesis and structural analysis of the corresponding dicobalt–alkyne complex derived from 9-ethynylfluoren-9-ol is also known [69].

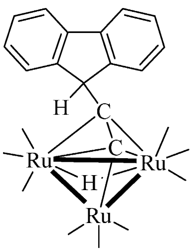

60

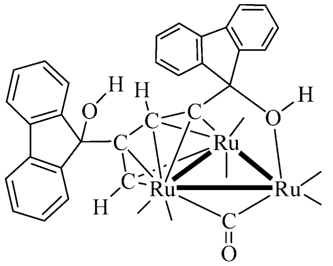

61

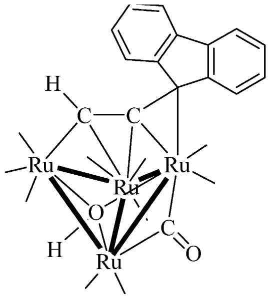

62

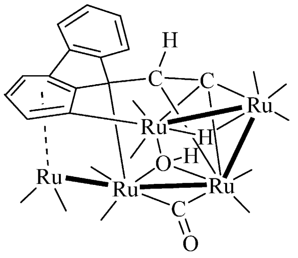

63

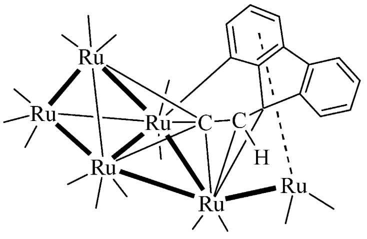

64

CO groups are omitted for clarity

3.1.2. N-donors

Fluorene-bridged dipyridyl ligands were prepared as useful building blocks for the construction of soluble macrocyclic supramolecules with different geometries by the self-assembly processes. They undergo facile ring closure reactions with $[Re(CO)_5X]$ (X = Cl, Br) to form trimetallic triangles **65** [70]. These supramolecules display emission of different origins that are triggered by the bridging aromatic segment. Emission was observed only at low temperature, and they show $^3(\pi\pi^*)$ and ^{3}MLCT-based emissions with prolonged lifetimes.

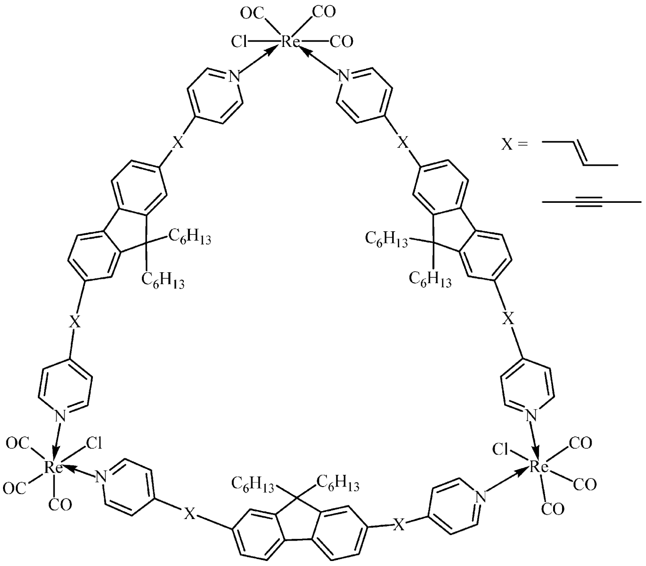

65

In a related context, the ligand **66** was shown to be capable of incorporating into infinite one-dimensional coordination polymers and square-grid polymer structures. Exceptionally large, non-interpenetrating, square-grid polymers $[Cu(\mathbf{66})_2(NO_3)_2]$ with grid dimensions of 25 Å × 25 Å were prepared [71]. The ABAB stacking of the layers generates reduced, yet still very large, infinite channels of dimensions 16 Å × 16 Å. Bunz and co-workers also accomplished the first chiral non-interpenetrating square-grid coordination polymers $[Cu(\mathbf{67})_2(NO_3)_2]$ derived from a chiral fluorene-based ligand **67**. The crystal of $[Cu(\mathbf{67})_2(NO_3)_2]$ crystallizes in the space group $P2_1$ and the grid dimension is still 25 Å × 25 Å [71]. But, the ABCABC stacking significantly reduces the accessible channel dimensions to about 8 Å × 8 Å. Along the same line, two luminescent coordination polymers with a triple-helix structure $[HgX_2(\mathbf{66})]_\infty$ (X = Cl, Br) **68** can be synthesized from HgX_2 and **66** [72]. The mercury atom lies in a distorted tetrahedral environment. There is a large shift in the emission between the free ligand and the coordination polymers. The intervening mercury atoms, which exert a strong electron-withdrawing effect as a consequence of their +2 charge and attached halides, have a significant influence on the fluorescent properties of the organic ligand.

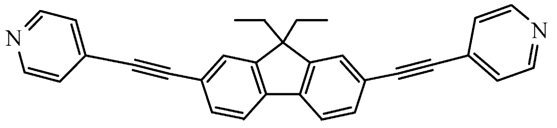

66

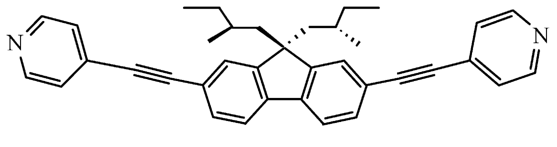

67

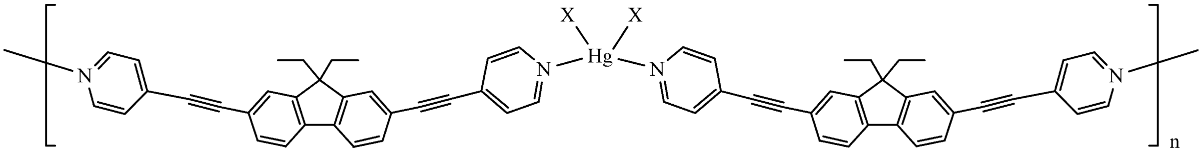

68 X = Cl, Br

Fluorene-containing bidentate bipyridine ligands, which could serve as models for the polymeric analogues possessing alternating fluorene and bipyridine units, were prepared and used as complexing agents for a variety of transition metals [73]. New octahedral complexes **69**–**74** were thoroughly characterized by NMR, FABMS, electronic and fluorescence spectra as well as CV measurements. The ferrocene-tethered fluorenyl bipyridine leads to novel heterobimetallic components. Except for the ferrocene-containing compounds, these metal complexes are luminescent at room temperature. The luminescence in the d^6 ruthenium complexes likely arises from an MLCT state, and fluorescence due to the ligand is completely quenched. When compared to $[Ru(bipy)_3]^{2+}$, these ruthenium complexes exhibit longer lifetimes, which probably stems from the delocalization of charge into the extended fluorene conjugation.

The use of bis-monodentate tectons based on the fluorene skeleton bearing two pyridine moieties **75** and **76** in a “V” shape geometry to form coordination networks in the presence of metal salts was described [74]. A neutral 1D coordination network is generated upon self-assembly of the tecton **75** with the metallatecton $HgCl_2$. By self-assembling of **76** with $CoCl_2$, a neutral 2D coordination network is obtained instead.

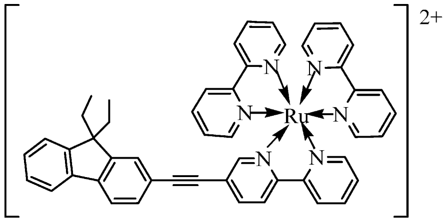

69

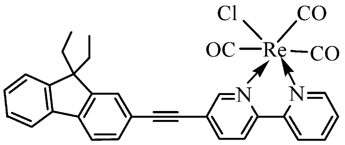

70

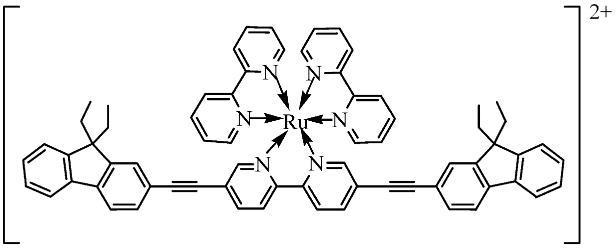

71

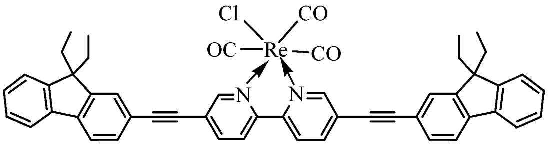

72

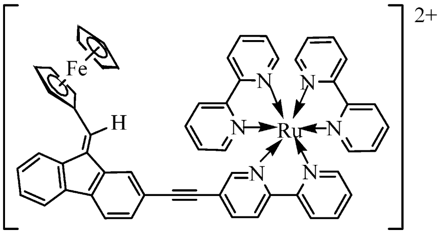

73

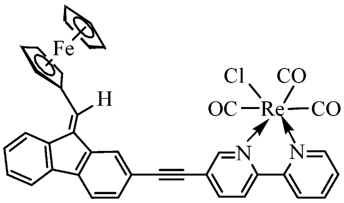

74

The synthesis and structural characterization of the first gold(I) cyanamide complex were reported by Adams [75].

Cyanamides are pseudo-halide nitrogen ligands that can readily be coordinated to metals. Compound **77** exhibits the ν(N=C=N) absorption at 2159 cm^{-1}, with a shoulder at 2123 cm^{-1}. The lowest energy absorption band at 483 nm in CH_2Cl_2 was assigned to an intramolecular charge-transfer from the cyanamide moiety to the fluorenone π skeleton.

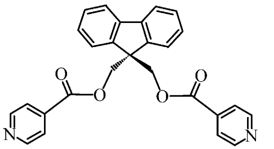

75

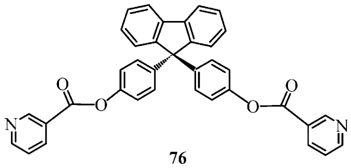

76

Three alternating polymers based on 2,2′-bipyridyl and fluorene units **78–80** were prepared and were shown to be responsive to a wide variety of transition metal ions such as Mn^{2+} through their absorption spectral red-shift and fluorescence quenching [76]. However, a clear difference in the sensing sensitivity was observed among these three polymers, attributable to the difference of the backbone rigidity of the polymers. The C–C single bond linker in **78** provides the weakest resistance (i.e., the highest backbone flexibility) to the coplanarity of the two pyridine rings of 2,2′-bipyridyl unit during chelation with metal ions, thus showing the highest sensitivity. For **80**, the ethynylene linker, which presents the highest backbone rigidity, offers a bigger hindrance for the coplanarity of the bipyridyl unit, and gives the poorest response sensitivity to metal ions.

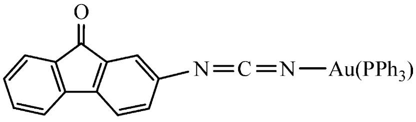

77

3.1.3. O-donors

Some europium(III) complexes with fluorene-functionalized β-diketone ligands **81** were synthesized and characterized by luminescence spectroscopy [77]. The authors studied the factors that improve the energy transfer efficiency between the host and the Eu guest as well as the volatility of these complexes.

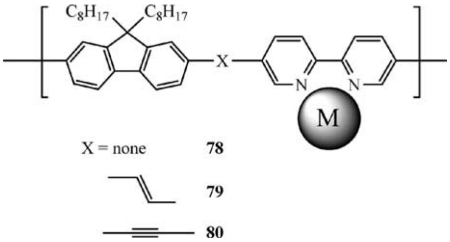

X = none **78**

79

80

A series of conjugated copolymers containing 9,9-dihexylfluorene and europium complex-chelated benzoate units **82** were synthesized through a three-step sequence, involving Suzuki coupling copolymerization, hydrolysis of benzoate units, and metal coordination [78]. These copolymers exhibited relatively high glass transition temperatures after incorporation of the Eu complexes. Intramolecular energy transfer from the fluorene groups to the europium complex takes place in dilute solutions. The PL spectrum of the copolymers shows two emission bands, one in the 350–550 nm region and another at around 612 nm, corresponding to the π–π^* transitions of the fluorene groups and the f–f transitions of the Eu^{3+} ions, respectively. However, the blue emission was significantly reduced in the solid state, and thus, nearly monochromatic red emission can be observed in some cases.

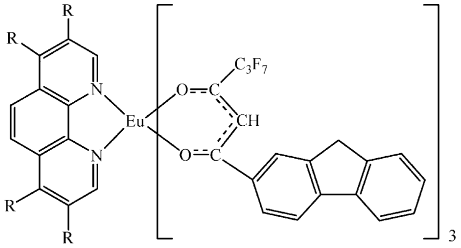

R = H, Me, Ph

81

High-efficiency red light-emitting electrophosphorescent PLEDs were fabricated using **83** by simultaneous incorporation of cyclometallated iridium complexes and charge transport moieties on the side chains of polyfluorene [79]. Energy transfer from an electroplex formed between fluorene main chain and side-chain carbazole moieties, in addition to that from the polyfluorene backbone, to the red iridium complex can markedly enhance the LED performance. Such devices can emit red light with an efficiency of 2.8 cd/A at 7 V and 65 cd/m^2.

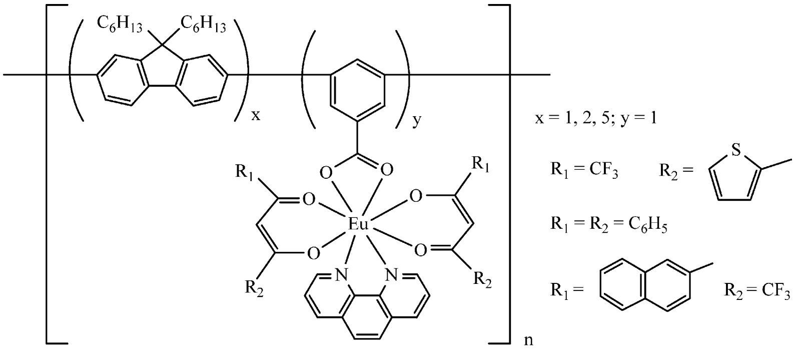

82

3.1.4. *Mixed C, N-donors*

A number of phosphorescent iridium(III) complexes with fluorene-modified phenylpyridine ligands **84–86** were prepared [80]. They are isolated as amorphous solids and thus are resistant to crystallization. Each of them shows weaker transitions red-shifted from the $^1(\pi\pi^*)$ band, corresponding to excitation to ^{1}MLCT, ^{3}MLCT and $^3(\pi\pi^*)$ states. Observation of the ^{3}MLCT and $^3(\pi\pi^*)$ bands confirms strong spin–orbit coupling. Complexes **84–86** can be used in the fabrication of single-layer LEDs. Modest efficiencies of 0.10, 0.04 and 0.07 cd/A were observed for **84–86**, respectively, for devices with a general architecture of ITO/PEDOT/Ir complex/Ca/Ag (PEDOT = poly(ethylenedioxythiophene)). In all cases, the quantum efficiencies are ca. 0.1%.

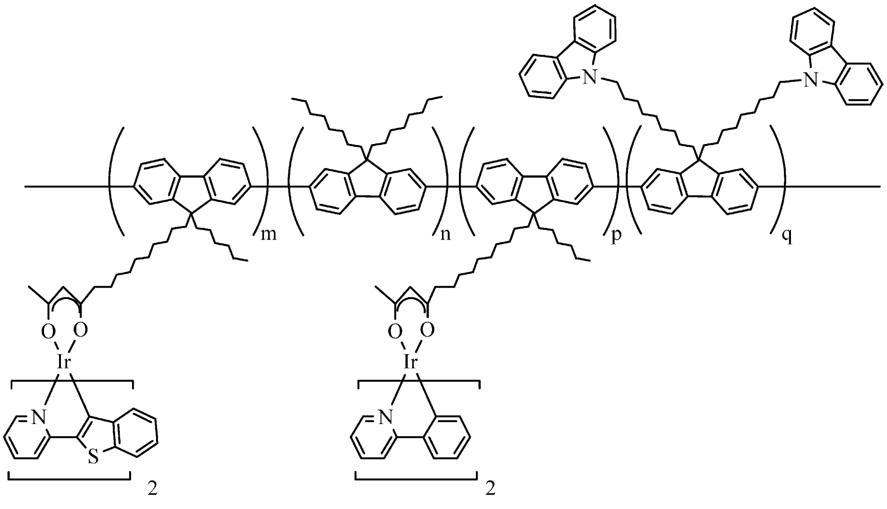

83

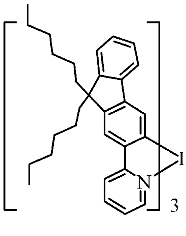

84

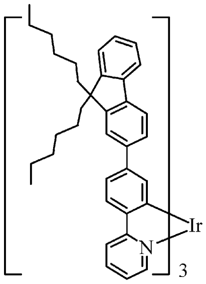

85

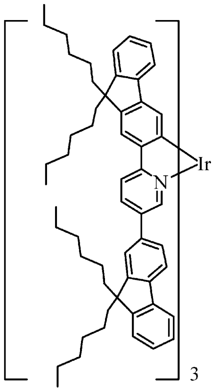

86

High-efficiency yellow–green electrophosphorescent OLEDs can be fabricated by doping **84** into a host polymer matrix of PVK blended with the electron-transporting 2-(4-biphenylyl)-5-(4-*tert*-butylphenyl)-1,3,4-oxadiazole (PBD) [81]. The highest external quantum efficiency was 10% photons/electron (ph/el) at a concentration of 0.3 wt.% **84** in PVK-PBD (40 wt.%). The highest luminous efficiency of 36 cd/A was observed (power efficiency of 2.5 lm/W) at 45 V. Brightness in excess of 8000 cd/m^2 was achieved at 75 mA/cm^2 (55 V). Emission from the dopant molecules in such devices involves localization of the injected electron and hole on the metal–organic center. This can occur by a variety of mechanisms, including Förster and/or Dexter energy transfer from the host transport material to the dopant, and direct trapping of both electrons and holes on the metal–organic group. No evidence of phase separation in the films of the devices was revealed by TEM. The same research team also reported electrophosphorescence from a polymer guest–host system with **85** as the guest and a blend of PVK and PBD as the host [82]. The LEDs turn on at ∼10 V and emit green light at 550 nm. An external quantum efficiency of 8% ph/el and luminous efficiency of 29 cd/A were achieved at 1 wt.% concentration of **85**. The devices exhibited no emission from PVK or PBD, even at the lowest concentration of **85** (0.1 wt.%). The results reveal that Förster energy transfer plays a minor role in achieving high efficiencies in these devices. Direct charge trapping appears to be the main operating mechanism. Along the same line, these authors also demonstrated red electrophosphorescent LEDs with high brightness and promising operational stability fabricated by blending **86** with the copolymer host, poly(9,9-dihexylfluorene)-co-2,5-dicyanophenylene [83]. The maximum luminance was 2200 cd/m^2. Devices with 1 wt.% **86** exhibited external quantum efficiency and luminous efficiency of 1.5% ph/el and 3 cd/A, respectively, at 142 cd/m^2.

3.2. *Carbazole groups*

Developments based on the exploitation of carbazole, a structural analogue of fluorene, as the building unit for the synthesis of branched molecules, oligomers, polymers or even dendrimers have recently aroused much attention, however, most of them are confined to organic systems [84–90]. It is well-known that carbazole group is a good hole-transporting unit and poly(*N*-vinylcarbazole) and related polymers containing carbazole moieties are especially

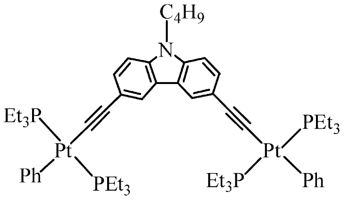

87

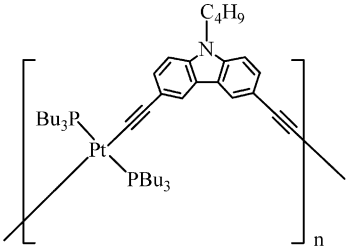

88

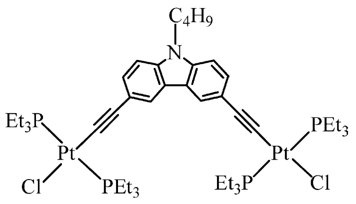

89

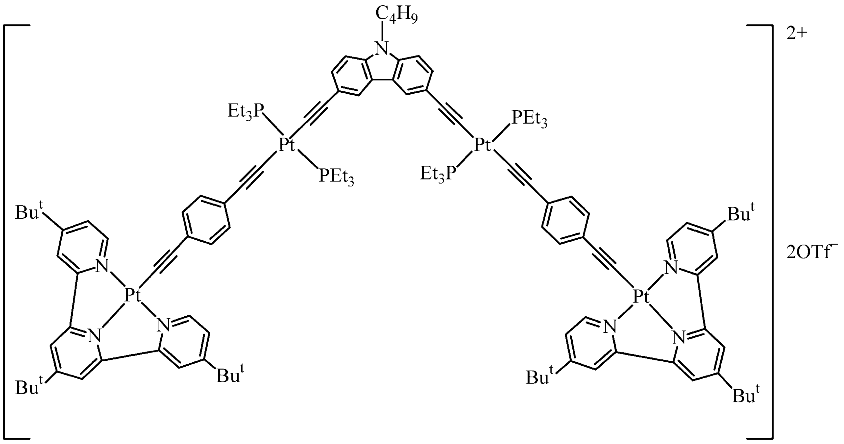

90

important charge transport polymers for OLEDs and as photorefractive materials for electrooptic devices. The following section will highlight recent advances in the synthesis and properties of metal compounds of carbazoles.

3.2.1. *C-donors*

To our knowledge, carbazole-containing metal alkynyl compounds are very rare in the literature. The first examples are the platinum(II) diyne **87** and polyyne **88** prepared through the CuI-catalyzed dehydrohalogenation between the platinum(II) chloride precursors and 9-butyl-3,6-diethynylcarbazole [49]. The regiochemical structure of polymer **88** has been ascertained by single-crystal X-ray analysis on the model complex **87**. Similar to other related systems, there is a red-shift in the absorption bands from the free alkyne to the platinum complexes and the transition energies of the polymer are lowered with respect to the dimer. It was shown that the S_1 singlet excited state extends over more than a repeat unit while the T_1 triplet state remains localized to less than one repeat unit. The bandgap measured is ca. 3.10 eV. The emission patterns of **87** and **88** are very similar and consist of a fluorescence peak at ~425 nm and a phosphorescence band at ~460 nm, both of which are π–π^* ligand-centered. The study indicates that the use of carbazole unit leads to high-energy triplet states and represents an effective approach in the enhancement of the ISC rate and hence the triplet emission. Polymer **88** was also shown to be a photoconducting material in a single-layer architecture with a photocurrent quantum efficiency of approximately 0.01% in the forward bias mode. More recently, Yam et al. have reported the synthesis, electrochemistry, luminescence studies and structural characterization of **89**. This complex, with two terminal chloro ligands, can serve as versatile building block for the assembly of a novel tetranuclear complex **90** [91]. Complex **90** can also be made via a divergent route from **89** in three steps. The CV of **90** shows two quasi-reversible terpyridine-based reduction couples together with three irreversible anodic waves corresponding to the metal-centered oxidations of the platinum diethynylcarbazole moiety and the [Pt(^{t}Bu$_3$-terpy)] units in the molecule. Comparison of the emission data of **90** with the starting precursors was made. Similar to the electronic absorption studies, the emission of **90** is likely to arise from an excited state of mixed ^{3}MLCT/^{3}LLCT character, involving a charge transfer from the platinum diethynylcarbazole unit to the terpyridyl part of the molecule and this was supported by electrochemical investigations.

3.2.2. *N-donors*

It is also common that the carbazole ligand behaves as an amido group in organometallic chemistry which coordinates to metals via the formation of M–N σ-bonds. This type of amido ligation using the carbazole group is believed to be a weaker π donor than the dialkylamido ligand because of the presence of the two coplanar aryl rings that would decrease nitrogen-p to metal-d π-donation. The metals that can form these complexes span from main group metals to transition metals as well as f-block elements.

X-ray structures of three alkaline-earth metal amides [(*N*-carbazolyl)$_2$Ca(pyridine)$_4$] **91**, [(*N*-carbazolyl)$_2$Sr(NH$_3$)(DME)$_2$] (DME = 1,2-dimethoxyethane) and [(*N*-carbazolyl)$_2$Ba(DME)$_3$] were reported [92]. They all crystallize as monomers with the M^{2+} cation (M = Ca, Sr, Ba) σ-bonded to the carbazole nitrogen atoms. While the metal coordination smoothly increases from six to seven to eight with M = Ca, Sr and Ba, respectively, the orientation of the anionic carbazole ligands changes from transoid for M = Ca, Sr to cisoid for M = Ba. The experimental structural data were correlated with theoretical results obtained by ab initio calculations and the covalent Ba–N σ-bonding contributions involving metal d-orbitals and cation polarization would favor bent X–Ba–X arrangements.

The chemistry of group 4 metals supported by carbazole hard donor ligation was studied by Rothwell and co-workers [93,94]. A series of derivatives of titanium and zirconium containing carbazole ligands have been isolated and structurally characterized. The bis(benzyl) complex **92** was prepared from [Ti(CH$_2$Ph)$_4$] and carbazole which can react with 2,6-dimethylphenyl isocyanide to give the bis(η^2-iminoacyl) complex **93**. Starting with the more bulky alkyl substrate [Ti(CH$_2$SiMe$_3$)$_4$], the alkylidene-bridged dimer **94** was obtained instead and subsequent reaction with 2,6-dimethylphenyl isocyanide produces **95** accompanied by the elimination of one molar equivalent of free carbazole [93,94]. An alternative approach using potassium carbazolate also affords two additional Ti(IV) compounds **96** and **97** from [CpTiCl$_3$] [94]. The same authors also reported the synthesis and characterization of zirconium compounds **98** and **99** [94]. Structural studies of **98** show that the Zr–N(carbazole) distances are 0.15 Å longer than the Zr–NMe$_2$ distances which is consistent with almost negligible nitrogen-p to metal-d π-bonding from the carbazole ligands.

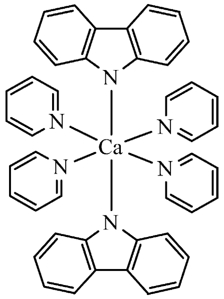

91

Several alkylidyne-bridged complexes of group 5 niobium and tantalum **100**–**103** have been prepared and their solid-state structures show the central 1,3-dimetallacyclobutadiene core supported by the four donor carbazole ligands [95]. Hydrogenation of the tantalum compound **102** in the presence of PMe$_2$Ph leads to the complex **104** [96] while both **100** and **102** react thermally with one equivalent of alkynes Me$_3$SiC≡CH and EtC≡CEt to form organometallic derivatives **105**–**108**, in which insertion of an alkyne unit into one of the alkylidyne bridges occurs to give non-planar six-membered dimetallacycles [97]. The reactions of **100** and **102** with organic isocyanide to give **109** and **110** were also examined which involve coupling of the isocyanide molecule with one of the alkylidyne bridges to result in an amido-alkyne unit [95].

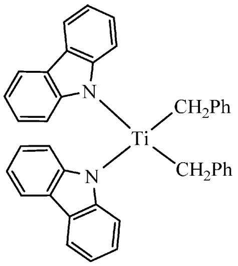

92

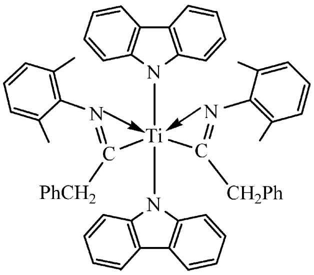

93

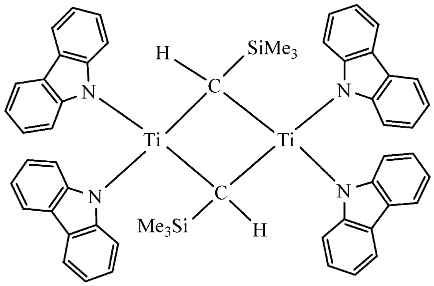

94

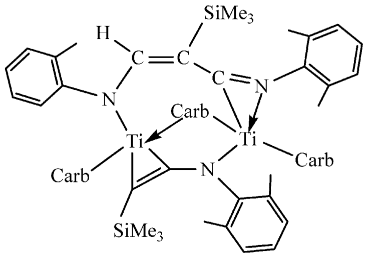

95

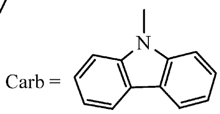

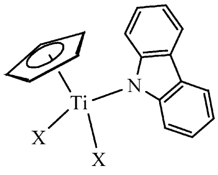

X = Cl **96**
X = Me **97**

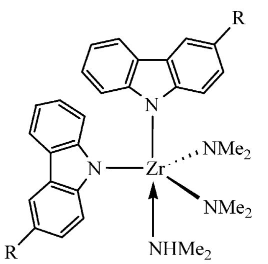

R = H **98**
R = ^{t}Bu **99**

The synthesis of the complex $2[\mathrm{Li(THF)_4}]^+[\mathrm{Cd(Carb)_4}]^{2-}$ **111** from the nucleophilic substitution reaction of $[\mathrm{Cd(NSiMe_3)_2}]$ with lithium carbazolate, Li(Carb), exemplifies a new, halide-free and general route to metallo-organic complexes [98]. A low-temperature X-ray diffraction experiment shows that complex **111** has an ion-separated structure which contains a tetraorganocadmiate dianion with the four carbazolate ligands attached in a tetrahedral geometry around the Cd center.

The utility of the carbazolate anion derived by deprotonation of carbazole as a monohapto ligand for lanthanoid(II) cations has been examined. These lanthanoid(II) organoamides are potentially useful synthetic reagents which could exert more regio- and stereochemical control than is possible with halides. The syntheses and crystal structures of several lanthanoid(II) carbazolate complexes **112–114** were reported [99–101].

The europium(III) complex **115** functionalized with a hole-transporting carbazole group was synthesized and used as a red emitter in a multilayered EL application [102]. Complex **115** basically emits the characteristic line-like spectrum from $\mathrm{Eu^{3+}}$ ion at 612 nm due to $^5\mathrm{D}_0 \rightarrow {}^7\mathrm{F}_2$ 4f electronic transition. Since no luminescence band from the carbazole-substituted 1,10-phenanthroline ligand can be observed, the energy absorbed by this ligand is transferred to the complex completely. OLED devices fabricated using **115** as the emitting layer show greatly enhanced performance, stability and operating repeatability. The results indicate that incorporation of hole-carrier functional entity into metal complex is an excellent strategy for modifying the hole-transporting characteristic of lanthanide complexes.

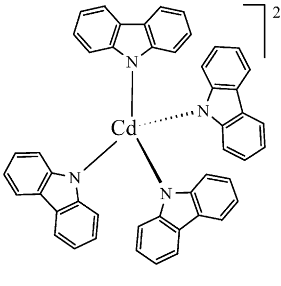

111

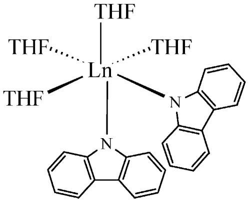

Ln = Sm, Eu

112

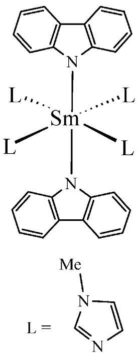

113

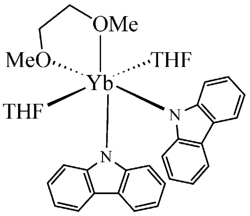

114

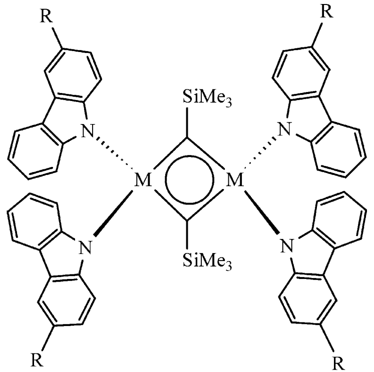

M = Nb, R = H **100**; R = ^{t}Bu **101**
M = Ta, R = H **102**; R = ^{t}Bu **103**

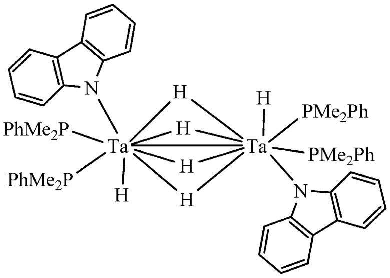

104

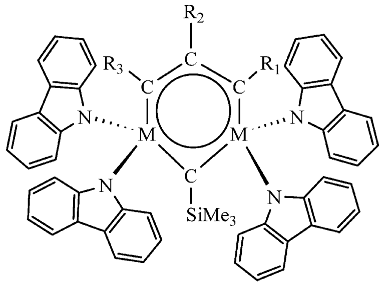

$\mathrm{R_1 = Me_3Si, R_2 = H, R_3 = Me_3Si}$, M = Nb **105**; M = Ta **106**
$\mathrm{R_1 = Me_3Si, R_2 = R_3 = Et}$, M = Nb **107**; M = Ta **108**

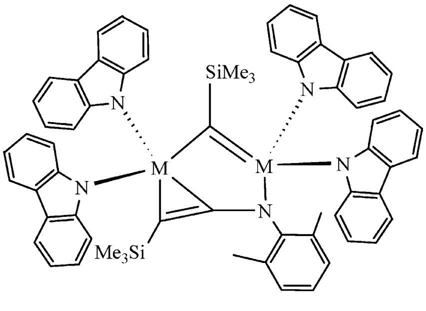

M = Nb **109** M = Ta **110**

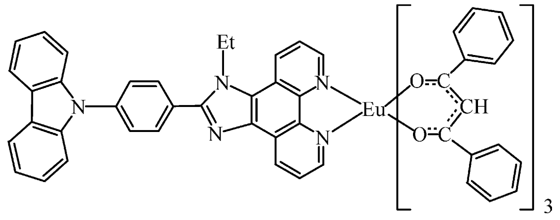

115

The synthesis, characterization and magnetic properties of some cobalt, iron and manganese complexes **116** and **117** derived from the tridentate bis(imino)carbazoles were described [103]. All of these 1,8-bis(imino)carbazolide products are paramagnetic and generally exhibit magnetic moments consistent with high spin configurations. The reactivities of the Fe and Co complexes with Ag(I) salts to give cationic derivatives and with MeLi to give metal-methyl compounds were also investigated.

Carbazole-linked ditopic pyridyl ligands, prepared by using a series of Sonogashira and Heck coupling reactions, are found to be useful synthons for the synthesis of soluble macrocyclic supramolecules by self-assembling with [Re(CO)$_5$X] (X = Cl, Br) to form the cyclic dimers **118** [70]. The molecular weights of these compounds were confirmed by FAB-MS. These carbazole-containing cyclic dimers are potentially novel photoactive materials and emit green light that probably arises from a ligand-localized $^1(\pi\pi^*)$ excited state.

The synthesis and characterization of carbazole-containing ruthenium complexes linked by an acetylene spacer **119** and **120** were also reported [104]. The ground state electronic properties of these compounds were examined by CV technique and absorption spectra. The excited state behavior was investigated after pumping the carbazole moiety. The presence of the Ru^{2+} unit strongly suppresses the fluorescence of the carbazole chromophore in both **119** and **120**. In the case of **119**, both Ru^{2+} and Ru^{3+} compounds (the latter being obtained by chemical or electrochemical oxidation) show a decrease of the fluorescence of carbazole, typical of other pentaammine complexes.

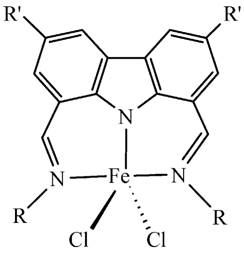

R = 2,4,6-Me$_3$C$_6$H$_2$, R' = Me, ^{t}Bu
R = Ph, R' = Me
R = ^{i}Pr, R' = Me

116

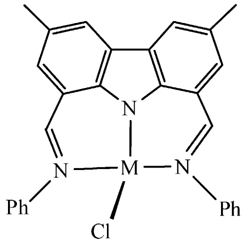

M = Mn, Fe, Co

117

The dendritic ligands of the first and second generations made of 1,10-phenanthroline coordinating subunits and of carbazole groups as branching sites can be used to form luminescent and redox-active Ru(II) complexes **121–123** [105]. The absorption spectra, luminescence properties and electrochemical behavior of these metal dendrimers were thoroughly studied and the results were compared to those of the free dendritic ligands. MLCT bands typical of other Ru(II) polypyridine complexes dominate the visible

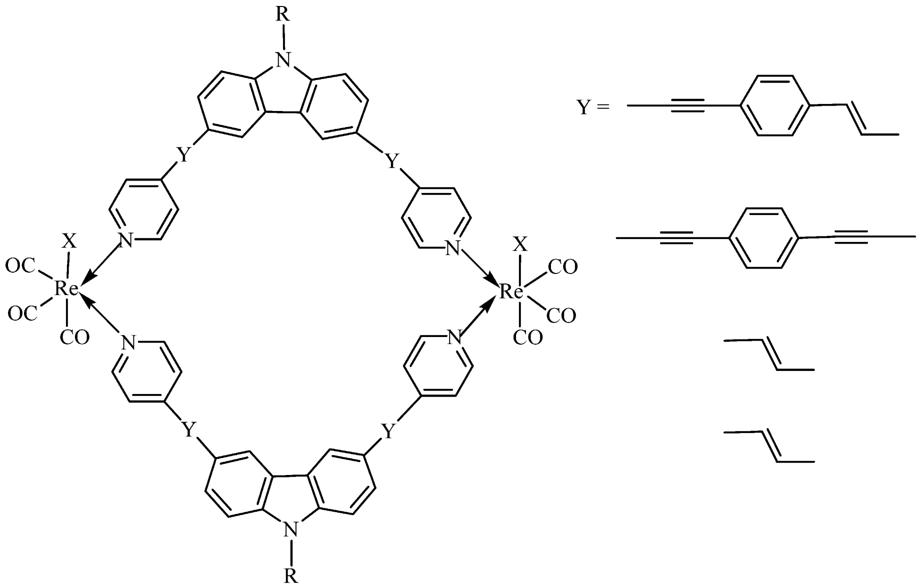

R = C$_6$H$_{13}$, X = Br
R = C$_6$H$_{13}$, X = Br
R = C$_6$H$_{13}$, X = Br
R = Ph, X = Cl

118

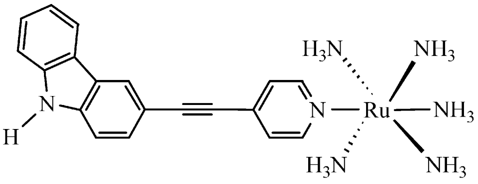

119

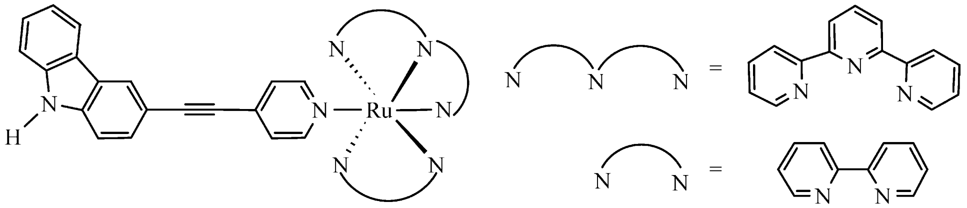

120

absorption spectra of these complexes, and formally triplet MLCT levels govern the excited state properties. Excitation spectroscopy shows that all the light energy absorbed by the dendritic branches is transferred with unitary efficiency to the emissive MLCT states in **121–123**, suggesting that these metal dendrimers are efficient light-harvesting antenna systems. Cyclic voltammetry data reveal that the Ru(II) complexes undergo reversible carbazole- and metal-centered

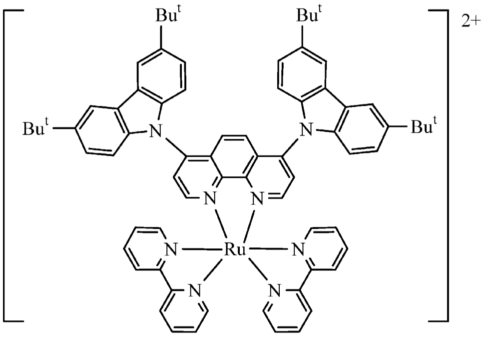

121

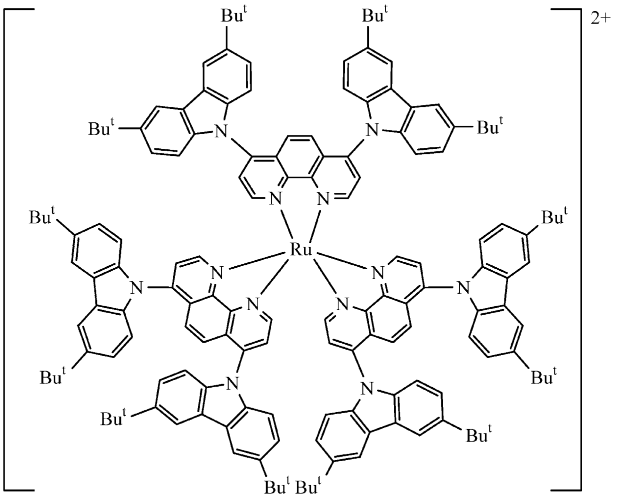

122

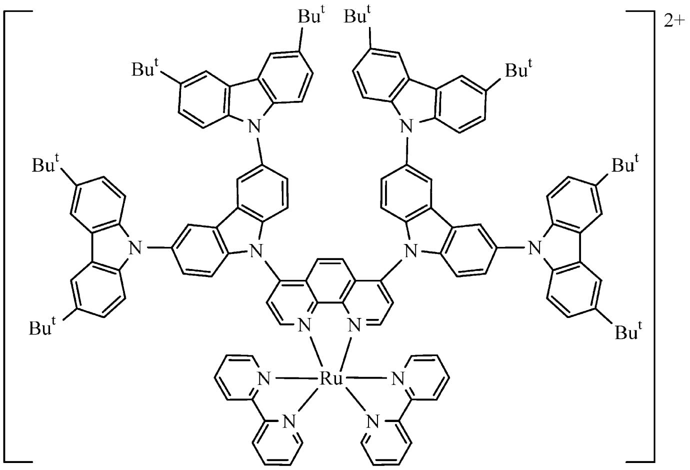

123

oxidation and polypyridine-centered reduction processes. The electronic interaction between the carbazole redox-active sites of the ligands is influenced by Ru(II) coordination.

A novel dinuclear ruthenium(II) complex **124**, which shows impressive on–off emission switching and strong binding to calf thymus DNA, was synthesized and photophysically characterized [106]. The effects of pH on UV–vis absorption and emission spectra of this complex were examined, and ground- and excited-state ionization constants were obtained. The binding studies were achieved by using absorption and luminescence titrations, steady-state emission quenching, and viscosity measurements. The authors found that the maximum on–off ratio is ∼100 over a narrow pH range of pH 8.0–10.0.

A novel synthetic route to carbazole-rich dendrimers containing the imine coordinating sites **125** was developed via cyclotrimerization [107]. These molecules were shown to be able to trap metal ions such as Sn^{2+} and Eu^{3+} through the formation of phenylazomethine-metal unit, giving rise to a change in the fluorescence characteristics. The degree of energy transfer can be controlled by the complexation process.

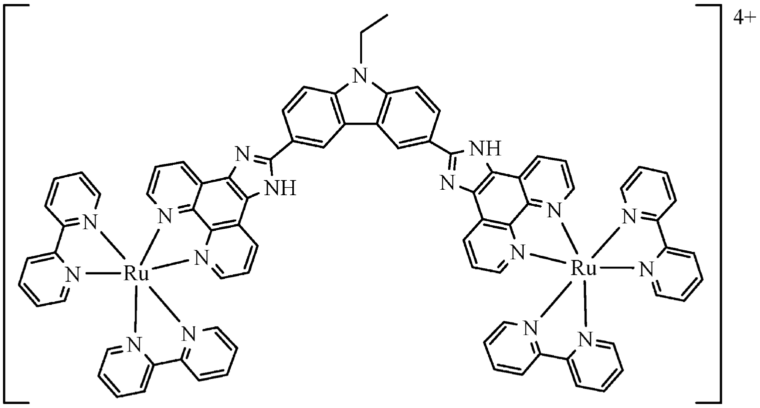

124

3.3. 4,5-Diazafluorene groups

The 4,5-diazafluorene ligands (dafe and dafo) differ from the parent fluorenes (fe and fo) by the replacement of the CH groups in the latter with N atoms. These have several distinct properties compared to their analogues 2,2′-bipyridine (bpy) and 1,10-phenanthroline (phen) (Fig. 8). Likewise, there are clear distinctions in the coordinating and bonding properties between dafe (or dafo) and bpy (or phen). For dafe, the methylene bridge in such 3,3′-annelated-2,2′-bipyridine distorts the bipyridine portion of the molecule and the increase in the bite angle will reduce the metal–nitrogen overlap. Hence, dafe is a weaker σ-bonding ligand than bpy. This is expected to promote dissociation of one of the donor N atoms, and result in an enhancement of opportunity for the formation of labile binuclear complexes which could be catalytically active. Dafe is effectively lower than bpy in the spectrochemical series which translates into an energetic lowering of any ligand-field (LF) states. Dafo is a modified bpy or phen ligand which contains a five-membered exocyclic ring bearing a reactive keto function. The two coordinating N atoms in dafo have a larger bite distance (2.99 Å) compared to phen (2.65 Å) which would produce unusual coordination modes and result in different redox and biological properties.

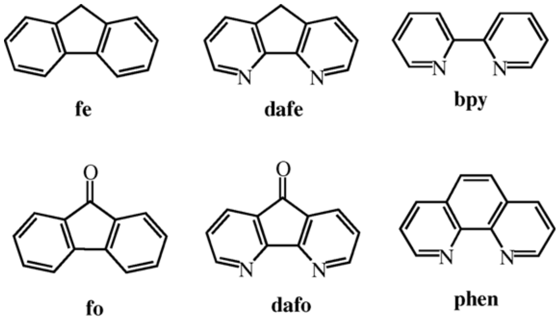

Fig. 8. Structures of some 3,3′-annelated-2,2′-bipyridine ligands and their analogues.

Some ruthenium(II) complexes of the form $[Ru(bpy)_2(L)](PF_6)_2$ (L = dafe and dafo) were prepared and photophysically characterized [108]. The crystal structure of $[Ru(bpy)_2(dafe)](PF_6)_2$ determined is isomorphous with $[Ru(bpy)_3](PF_6)_2$ and has crystallographic symmetry D_3, requiring the diazafluorene methylene group to be disordered into three positions with a population of 1/3. Comparison of the photophysical data of $[Ru(dafe)_3]^{2+}$ with $[Ru(bpy)_3]^{2+}$ supports the contention that MLCT states are not substantially affected by substitution of dafe for bpy and the π^* levels of the ligands are more critical in influencing the MLCT energies. It was suggested by the authors that this Ru(II) polypyridine complex has the lowest excited state characterized by mainly a LF configuration and in other words, the dafe ligand permits the selective perturbation of LF states. The application of this approach to these Ru(II) complexes indicates that the MLCT and LF states are in thermal equilibrium. Along the same line of research, Rillema et al. reported a series of Ru(II) complexes of the types $[Ru(bpy)_n(dafo)_{3-n}]^{2+}$ and $[Ru(bpy)_n(dafo\text{-}ketal)_{3-n}]^{2+}$ **126–128** ($n = 0$–3) and their photochemical, photophysical and electrochemical properties were investigated [109]. In each series, the visible absorption feature associated with the MLCT transition shows a blue-shift and the oxidation potential for the Ru(III)/Ru(II) couple becomes more positive as n decreases. The emission data of the series $[Ru(bpy)_n(dafo)_{3-n}]^{2+}$ identify the emitting state of the complexes to be on bpy portion of the dafo ligand, but not on the carbonyl moiety. It was shown that the emission quantum yields decrease in the orders $[Ru(bpy)_2(dafo)]^{2+} > [Ru(bpy)(dafo)_2]^{2+} > [Ru(dafo)_3]^{2+}$ and $[Ru(bpy)_2(dafo\text{-}ketal)]^{2+} > [Ru(bpy)(dafo\text{-}ketal)_2]^{2+} > [Ru(dafo\text{-}ketal)_3]^{2+}$.

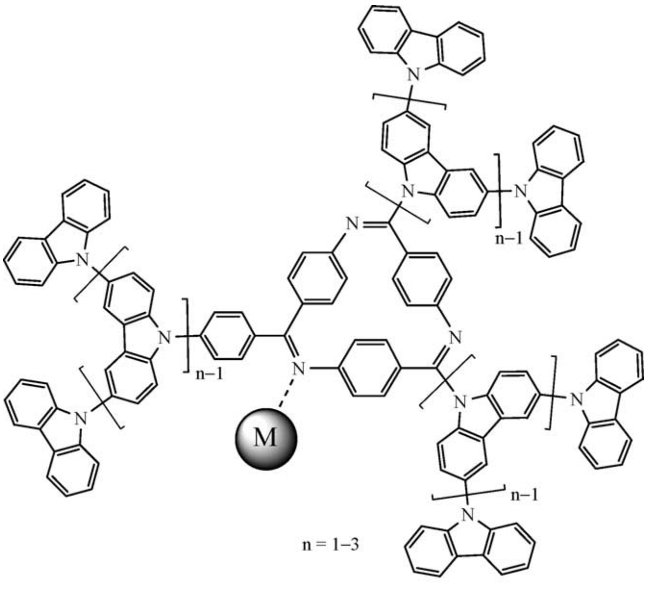

125

The interaction of $[Ru(phen)_2(dafo)]Cl_2$ with DNA was explored using a variety of biophysical and spectroscopic methods [110]. This metal–ligand complex appears to intercalate and surface-bind to DNA. The equilibrium binding constant as determined by equilibrium dialysis was $2.1 \times 10^3\ M^{-1}$ and all the binding parameters measured conform to a random non-cooperative model. Such studies can be useful in systematic studies of DNA recognition as well as that of other biopolymers.

A series of bimetallic complexes of ruthenium(II) with diazafluorene-based bridging ligands **129–132** were prepared and their redox and photophysical characteristics investigated [111]. Except for **132**, each of the complexes **129–131** shows one metal-based oxidation and four ligand-centered reduction waves. The effect of spacer length on the redox properties and the possible electrochemical pathways involved are discussed. These complexes give rise to MLCT absorptions in their visible spectra and intraligand $\pi \rightarrow \pi^*$ transitions in the UV spectra. The emission spectra of all of them at 77 K displayed vibrational components similar to those reported for $[Ru(bpy)_3]^{2+}$ and the emission maxima were all blue-shifted by ~0.034 eV relative to $[Ru(bpy)_3]^{2+}$. The positions of the emission energy maxima are relatively independent of the complexes studied at 77 K. Emission lifetimes at room temperature were obtained from extrapolation based on temperature-dependent lifetime measurements and are inversely related to the distances of the two Ru(II) centers of the dinuclear complexes: **129** (12.4 Å, 0.36 ns) > **130** (14.9 Å, 0.12 ns) > **131** (19.2 Å, 0.10 ns).

The synthesis, crystal structures and electrochemistry of the stable trigonal-bipyramidal copper(I) complex $[Cu(dafo)_2X]$ (X = Br, I, SCN) were discussed [112]. The SCN-bridged Cu(I) complex forms 2D sheets in the crystal, held together by weak interactions involving the dafo ketone group. As revealed by CV results, dafo can stabilize the Cu(I) oxidation state more efficiently than phen due to its better π-acceptor ability. The same research group also structurally and electrochemically characterized a neutral complex $[Cu(dafo)_2Cl_2][dafoH^+{\cdot}H_2O]_2(ClO_4)_2$ [113]. This complex can serve as a good model of ionic pockets with metal active sites in some metalloproteins. A related complex $[Cu(dafo)_2(H_2O)_2](ClO_4)_2$ was also crystallographically elucidated and shown to possess a 2D network structure linked up by hydrogen bonds [114]. The coordination chemistry of dafo and 9,9′-bis(4,5-diazafluorenyl) towards nickel(II), copper(II)

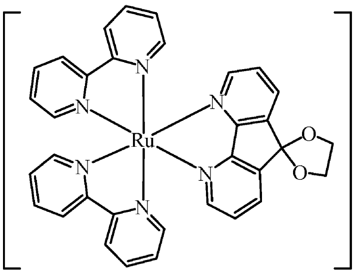

126

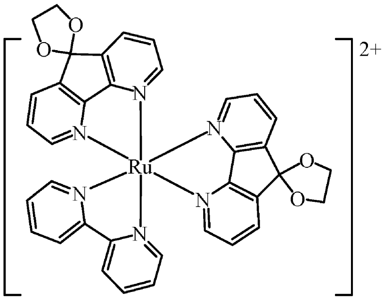

127

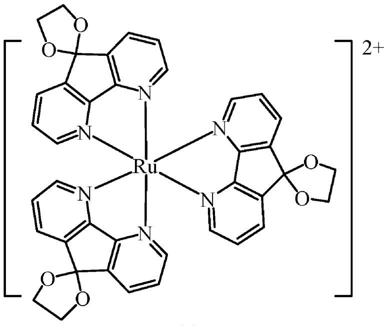

128

and zinc(II) was studied [115]. Steric strain of the ligand has no noticeable effect on their coordinating behavior with smaller 3d-metals. The seven-coordinate cadmium(II) compound [Cd(dafo)$_2$(PPh$_3$O)(CH$_3$COO)]ClO$_4$ **133** has been isolated in which the crystal structure shows a distorted monocapped trigonal prismatic coordination geometry [116]. A salient feature in **133** lies in the helical chains of cations induced by intermolecular π–π stacking interactions of dafo rings.

The copper(II) complex **134** containing 9-diazo-4,5-diazafluorene (dafeN$_2$) ligands was tested for its ability to cleave DNA photochemically [117]. Consideration of the experimental data leads to the conclusion that it is an effective DNA photocleaving agent that may be activated using visible light under hypoxic conditions. The activity is much lower for the ligand alone or when [Cu(dafo)$_2$(NO$_3$)$_2$] was used. Conductivity studies indicate that the NO$_3{}^-$ ions dissociate to form a 2:1 electrolyte in aqueous solution leaving a labile site that permits the DNA substrate to bind to the Cu center. A rare example of a tripodal copper(II) complex [Cu(tren)(dafeN$_2$)]$^{2+}$ **135** (tren = tris(2-aminoethyl)amine) was analyzed to possess an unusual (4 + 1 + 1′) structure, in which it has five stronger coordinated atoms and a weak semi-coordinated atom to give an asymmetric bidentate ligation [118]. Such a structure can be related to the associative complex in the ligand substitution reaction of [Cu(tren)L]$^{2+}$. The electronic and variable temperature EPR spectra in absolute DMF show that the two N atoms of dafeN$_2$ coordinate to the Cu(II) ion in a 2D fluxional model.

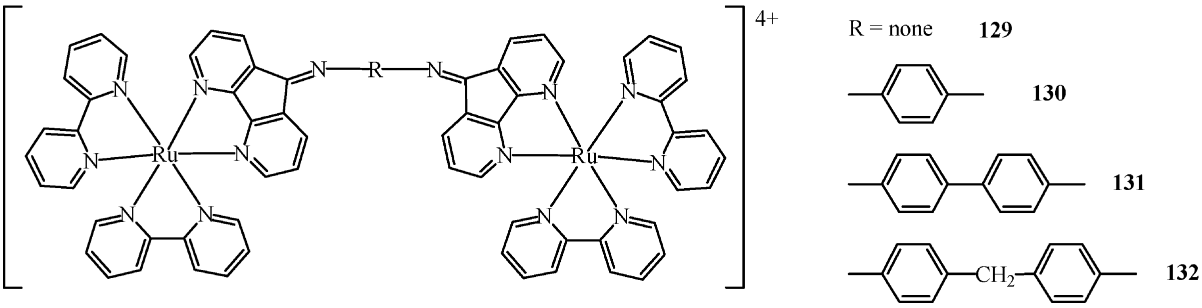

A family of zerovalent palladium-π-quinone complexes **136–138** showing monodentate or bridging coordination mode for the diazafluorenes has been synthesized and structurally characterized [119]. The type of products obtained depends on the type of substitution of the quinone used and the reactant stoichiometry. Such a difference in the coordination behavior is in line with the geometrical constraints of dafo and dafe which have a larger bite angle of 82° (77° for bpy). This system has also been partially extended to the platinum congeners.

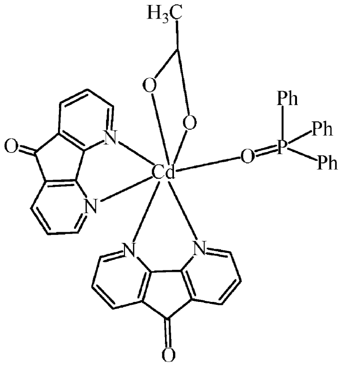

133

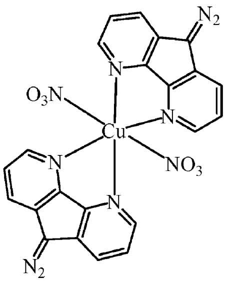

134

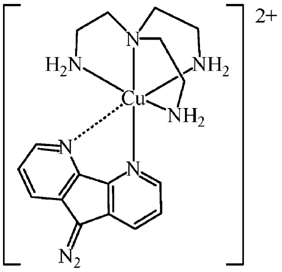

135

The preparations of sulfur-rich palladium complexes **139–142** were accomplished recently [120]. In the crystal structure of complex **139**, the planar molecules are further stacked forming two inequivalent columns with C· · ·C, S· · ·C and S· · ·Cl contacts. The differences between dichloro complexes and dmit complexes (dmit = 1,3-dithiole-2-thione-4,5-dithiolate) in their IR and UV data were discussed. Although the complexes themselves are insulators at room temperature, the iodine-doped compounds are semiconducting. Such doping process involves partial oxidation of complexes by I$_2$ to form ionic adducts with I$^-$ or I$_3{}^-$ anions.

A derivatized ligand 4,5-diazafluoren-9-one benzoylhydrazone, which tends to enolize from the keto-form in solution, can be used to complex with Co(OAc)$_2$ to give **143** [121]. This approach is also applicable to Mn(II), Ni(II), Cu(II), Zn(II) and Pb(II) ions. These metal complexes were fully characterized by common analytical and spectroscopic methods, molar conductivity measurements and TGA. Single-

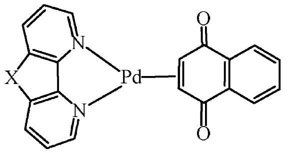

136

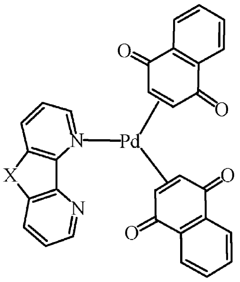

137

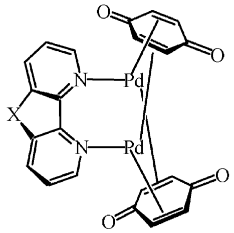

138

X = CH_2, CO

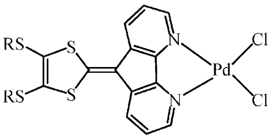

R = Me **139**
R-R = CH_2CH_2 **140**

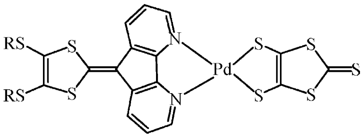

R = Me **141**
R-R = CH_2CH_2 **142**

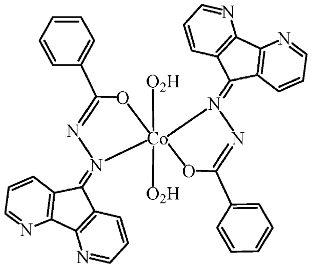

143

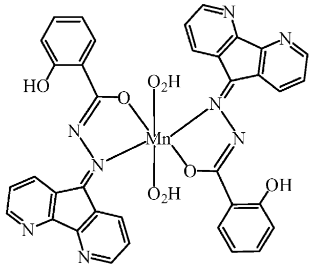

144

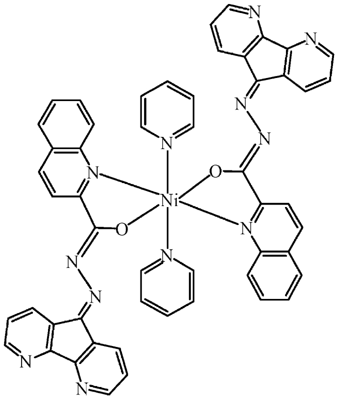

145

crystal X-ray structural analysis of **143** reveals that it has a centrosymmetric octahedral geometry which is stabilized by weak intermolecular interactions of both hydrogen bonds and π–π stacking between the diazafluorene moieties. A large electronically delocalized system throughout the whole molecule is thus formed after enolization and complexation. The authors also extended the same coordination chemistry to the 4,5-diazafluoren-9-one salicyloylhydrazone ligand and complexes such as **144** can be isolated [122]. The crystal structures of the Mn(II) and Co(II) complexes were determined. In both series, the non-coordination of the 4,5-diazafluorene unit shows that its chelating ability is weaker than the acylhydrazone group and it is likely that we can make use of the dangling N atoms for the construction of polynuclear complexes. On the other hand, the use of 4,5-diazafluoren-9-one quinaldinoylhydrazone in complex formation results in a novel coordination mode for Ni(II) as shown in **145** [123]. IR spectral and X-ray structural data confirm that complex **145** is octahedral and the molecules are stabilized by the intermolecular π–π stacking between the diazafluorene planes in adjacent molecules.

Interesting rhenium(I) surfactant complexes **146** and **147** bearing azo- and stilbene functionalities have been prepared and photophysically characterized [124]. The X-ray structure of **147** was established. Both complexes are found to exhibit reversible photoisomerization upon visible light irradiation. The presence of the Re(I) metal center allows an efficient

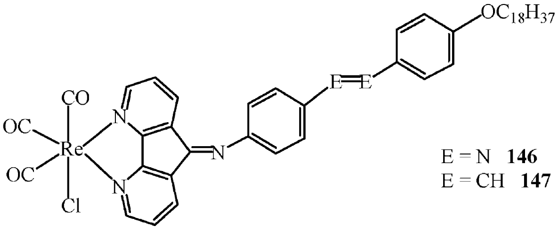

E = N **146**
E = CH **147**

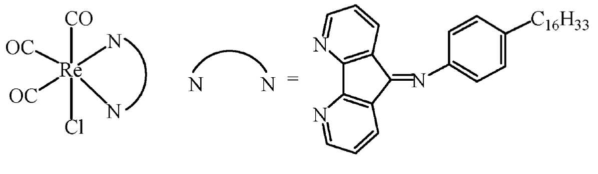

148

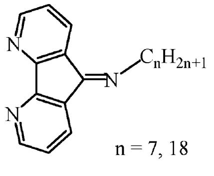

149

photosensitization pathway, i.e., intramolecular energy transfer from the ^{3}MLCT state to the ^{3}IL. Other Re(I) derivatives of the similar types **148** and **149** are also known. The formation and optical properties of their LB films were examined followed by a discussion of the second-harmonic generation (SHG) behavior [125].

Two amphiphilic ruthenium(II) surfactant molecules with long hydrocarbon chains **150** and **151** are demonstrated to show good monolayer and multilayer film-forming properties [126]. Both of them are SHG active with activities about 3.6 and 2.6 times of that of the organic standard (*E*)-*N*-methyl-4-(2-(4-octadecyloxyphenyl)ethenyl)pyridinium iodide.

Novel binuclear ruthenium(II) complexes with space-separated 4,5-diazafluorene moieties **152** and **153** were reported [127]. Cyclic voltammetry, differential pulse voltammetry and spectroelectrochemical studies on these Ru_2 complexes showed a single oxidation and no transient accumulation of a mixed-valence Ru^{II}, Ru^{III} state, thereby suggesting weak interaction between the metal termini. Metal complexes of Ru(II), Os(II) and Re(I) **154** containing a ligand system where a 4,5-diazafluorene-type chelate and a methoxybenzoxanthene unit are coupled by a double bond were prepared and their UV–vis spectroscopic data were recorded [128].

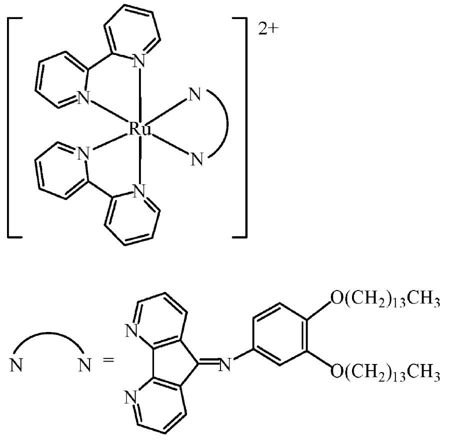

150

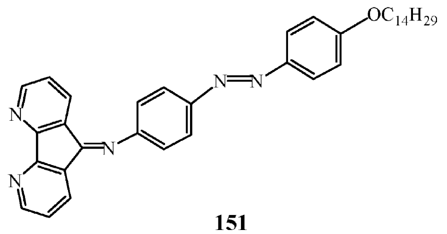

151

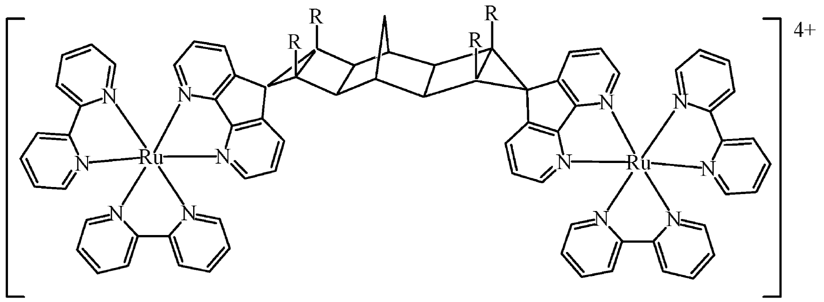

152

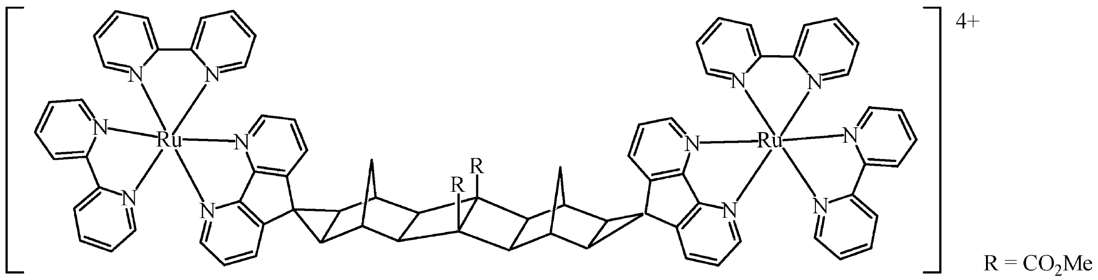

153

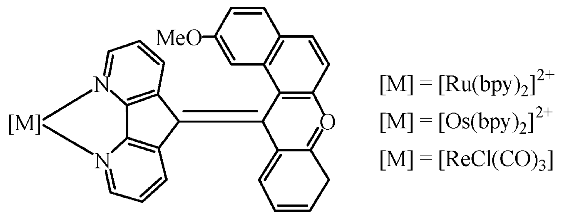

154

A series of first-row transition metal tris(chelate) complexes **155** with the 4,5-diazafluorene radical were isolated [129]. For Cu(II) ion, the reactions afforded products of different stoichiometries depending on the coordinating ability of the counterion. The magnetic properties of these compounds were examined at various temperature ranges and the experimental magnetic moments indicated non-interacting spins of the metal ion and the radicals at 200–300 K. At low temperatures, spin pairing of metal and radical spins is observed for Mn, Fe and Co ions. The formation of **156–158** from the reaction of $Cp'_2Ti(\eta^2-C_2(SiMe_3)_2)$ ($Cp' = C_5H_5$, C_5HMe_4 and C_5Me_5) with 4,5-diazafluorene involves an electron transfer from Ti to the fluorene unit accompanied by the release of one hydrogen atom from the sp^3 carbon atom of the ligand [130]. The crystal structure of **158** shows a pseudo-tetrahedrally coordinated Ti(III) center. These Ti compounds were fully characterized by EPR and electronic absorption spectroscopies. The presence of Ti(III) was unequivocally proven by the EPR spectra, showing typical features of Ti(III) derivatives. The absorption data of **156–158** in solution showed a well-resolved vibrational structure of the dafe anion with the positions of all vibronic bands shifted to longer wavelength by ca. 20–30 nm, and a low intensity band probably of the d–d transition in the range 820–940 nm.

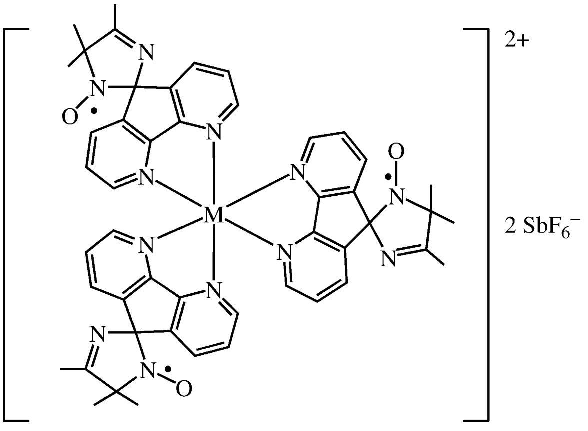

M = Mn, Fe, Co, Ni, Zn

155

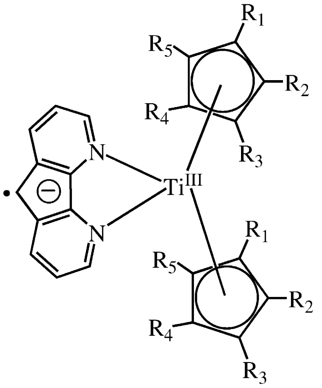

$R_1 = R_2 = R_3 = R_4 = R_5 = H$ **156**
$R_1 = H, R_2 = R_3 = R_4 = R_5 = Me$ **157**
$R_1 = R_2 = R_3 = R_4 = R_5 = Me$ **158**

4. Concluding remarks and perspectives

This article provides a comprehensive review of the synthesis, properties and applications of fluorene-derived transition metal complexes and polymers. The different classes of these materials are described according to their donor types. Plenty of examples covered here emphasize the richness and diversity in these areas of research. Although there were a number of excellent review articles dealing with the synthesis and materials properties of organic-based fluorene derivatives, it was not until recently that the parallel chemistry of well-characterized metal-based counterparts become a challenging field of endeavor in the research community. The past two decades have seen an ever-increasing interest in these compounds, especially in light of their important electrical, optical, catalytic, magnetic and luminescent properties. The wide ranges of synthetic methodologies combined with their remarkable applications are the main reasons for the rapid developments in this field. The studies summarized herein have realized great advances in the role played by the metal centers in governing the properties of fluorene derivatives. Almost all of the complexes which have been prepared with fluorene-, carbazole- and diazafluorene-containing bridges show rich luminescent and redox behavior. In the majority of cases, the versatility of preparing new metal complexes of fluorene derivatives has been demonstrated by insertion of different peripheral groups on the fluorene ring and variation of the 9-substituents can affect the optical and photophysical properties of these materials.

We believe that future research in this area will be focused on the in-depth exploration of these metal-based fluorene derivatives in optoelectronic studies and applications. Such research would provide a big step towards the creation of technologically useful materials for practical applications. An added bonus of incorporating transition metals into the organic structures is the possibility of harvesting energy from the triplet excited states and indeed, the exploration of triplet emitters for optoelectronics research has a great potential to excel in the next decade or so. It is envisioned that this could lead to the development of new electronic materials for molecular optoelectronics and photonics. It is certain that such work will excite scientists in both academic institutes and industry and make a major positive impact on the science and technology of organic optoelectronics through the creation of novel molecular materials. This line of research picks a timely topic with the potential for very high scientific and technological pay-off. In conclusion, it is clear that research into metal-fluorene complexes has a great deal to offer in many ways, particularly with regard to synthesizing novel complexes with unusual molecular topologies and/or unique physical properties. Virtually all the transition metals can be used to form such complexes. The design of new topological structures and arrays could lead to nanoscale materials with unique properties and these achievements would find possible future applications in nanoscale devices. The materials properties that are already known will continue to be focused upon and enhanced through greater processability and a better understanding of structure–property relationships. Greater control and design of molecular topologies and innovative chemical synthesis ensures a bright and exciting future for metal-fluorene compounds.

Acknowledgements

The author gratefully acknowledges financial support from the Research Grants Council of the Hong Kong SAR, PR China (Project Nos. HKBU 2048/01P and 2022/03P) and the Hong Kong Baptist University (FRG/01-02/II-48).

References

[1] T.A. Skotheim, R.L. Elsenbaumer, J.R. Reynolds, Handbook of Conducting Polymers, Marcel Dekker, New York, 1998.
[2] H. Shirakawa, Angew. Chem. Int. Ed. 40 (2001) 2574.
[3] A.G. MacDiarmid, Angew. Chem. Int. Ed. 40 (2001) 2581.
[4] A.J. Heeger, Angew. Chem. Int. Ed. 40 (2001) 2591.
[5] Y. Shirota, J. Mater. Chem. 10 (2000) 1.
[6] U. Mitschke, P. Bäuerle, J. Mater. Chem. 10 (2000) 1471.
[7] T. Yamamoto, Macromol. Rapid Commun. 23 (2002) 583.
[8] J.H. Burroughes, D.D.C. Bradley, A.R. Brown, R. Marks, N.K. Mackay, R.H. Friend, A.B. Holmes, Nature (London) 347 (1990) 539.
[9] J.R. Sheats, H. Antoniadis, M. Hueschen, W. Leonard, J. Miller, R. Moon, D. Roitman, A. Stocking, Science 273 (1996) 884.
[10] A. Kraft, A.C. Grimsdale, A.B. Holmes, Angew. Chem. Int. Ed. Ed. 37 (1998) 402.
[11] R.H. Friend, R.W. Gymer, A.B. Holmes, J.H. Burroughes, R.N. Marks, C. Taliani, D.D.C. Bradley, D.A. Santos, J.L. Brédas, M. Lögdlund, W.R. Salaneck, Nature (London) 397 (1999) 121.
[12] P. Nuguyen, P. Gómez-Elipe, I. Manners, Chem. Rev. 99 (1999) 1515.
[13] I. Manners, Synthetic Metal-Containing Polymers, Wiley, Weinheim, 2004, p. 153, Chapter 5.
[14] A.S. Abd-El-Aziz, Macromol. Rapid Commun. 23 (2002) 995.
[15] A.S. Abd-El-Aziz, E.K. Todd, Coord. Chem. Rev. 246 (2003) 3.
[16] C. Janiak, Dalton Trans. (2003) 2781.
[17] R.P. Kingsborough, T.M. Swager, Prog. Inorg. Chem. 48 (1999) 123.
[18] T.L. Stott, M.O. Wolf, Coord. Chem. Rev. 246 (2003) 89.
[19] D. Neher, Macromol. Rapid Commun. 22 (2001) 1365, and references cited therein.
[20] B. Tsuie, J.L. Reddinger, G.A. Sotzing, J. Soloducho, A.R. Katritzky, J.R. Reynolds, J. Mater. Chem. 9 (1999) 2189.
[21] K.-T. Wong, Y.-Y. Chien, R.-T. Chen, C.-F. Wang, Y.-T. Lin, H.-H. Chiang, P.-Y. Hsieh, C.-C. Wu, C.-H. Chou, Y.O. Su, J. Am. Chem. Soc. 124 (2002) 11576.
[22] W.-L. Yu, J. Pei, W. Huang, A.J. Heeger, Adv. Mater. 12 (2000) 828.
[23] S. Setayesh, A.C. Grimsdale, T. Weil, V. Enkelmann, K. Müllen, F. Meghdadi, E.J.W. List, G. Leising, J. Am. Chem. Soc. 123 (2001) 946.
[24] D. Marsitzky, R. Vestberg, P. Blainey, B.T. Tang, C.J. Hawker, K.R. Carter, J. Am. Chem. Soc. 123 (2001) 6965.
[25] S. Janietz, D.D.C. Bradley, M. Grell, C. Glebeler, M. Inbasekaran, E.P. Woo, Appl. Phys. Lett. 73 (1998) 2453.
[26] A.W. Grice, D.D.C. Bradley, M.T. Bernius, M. Inbasekaran, W.W. Wu, E.P. Woo, Appl. Phys. Lett. 73 (1998) 629.
[27] W.-L. Yu, Y. Pei, Y. Cao, W. Huang, A.J. Heeger, Chem. Commun. (1999) 1837.
[28] N.G. Pschirer, U.H.F. Bunz, Macromolecules 33 (2000) 3961.
[29] U. Scherf, E.J. List, Adv. Mater. 14 (2002) 477.
[30] D.D. Mysyk, I.F. Perepichka, D.F. Perepichka, M.R. Bryce, A.F. Popov, L.M. Goldenberg, A.J. Moore, J. Org. Chem. 64 (1999) 6937.
[31] I.F. Perepichka, A.F. Popov, T.V. Orekhova, M.R. Bryce, A.M. Andrievskii, A.S. Batsanov, J.A.K. Howard, N.I. Sokolov, J. Org. Chem. 65 (2000) 3053.
[32] P.J. Skabara, I.M. Serebryakov, I.F. Perepichka, N.S. Sariciftci, H. Neugebauer, A. Cravino, Macromolecules 34 (2001) 2232.
[33] I.F. Perepichka, in: F. Kajzar, M.V. Agranovich (Eds.), Multiphoton and Light Driven Multielectron Processes in Organics: Materials, Phenomena, Applications. NATO Science Series: 3. High Technology, vol. 79, Kluwer Academic, Dordrecht, 2000, p. 371.
[34] N.I. Sokolov, Y.M. Barabash, I.V. Poperenko, I.F. Perepichka, D.D. Mysyk, V.A. Komarov, Funct. Mater. 5 (1998) 441.
[35] N.J. Long, C.K. Williams, Angew. Chem. Int. Ed. 42 (2003) 2586.
[36] V.W.-W. Yam, Acc. Chem. Res. 35 (2002) 555.
[37] P.J. Low, M.I. Bruce, Adv. Organomet. Chem. 48 (2001) 71.
[38] W.-Y. Wong, G.-L. Lu, K.-F. Ng, C.-K. Wong, K.-H. Choi, J. Organomet. Chem. 637–639 (2001) 159.
[39] W.-Y. Wong, K.-Y. Ho, K.-H. Choi, J. Organomet. Chem. 670 (2003) 17.
[40] W.-Y. Wong, K.-Y. Ho, S.-L. Ho, Z. Lin, J. Organomet. Chem. 683 (2003) 341.
[41] W.-Y. Wong, G.-L. Lu, K.-H. Choi, Z. Lin, Eur. J. Org. Chem. (2003) 365.
[42] S. Takahashi, Y. Kuroyama, K. Sonogashira, Synthesis (1980) 627.
[43] A.J. Moore, A. Chesney, M.R. Bryce, A.S. Batsanov, J.E. Kelly, J.A.K. Howard, I.F. Perepichka, D.F. Perepichka, G. Meshulam, G. Berkovic, Z. Kotler, R. Mazor, V. Khodorkovsky, Eur. J. Org. Chem. (2001) 2671.
[44] D.F. Perepichka, I.F. Perepichka, A.F. Popov, M.R. Bryce, A.S. Batsanov, A. Chesney, J.A.K. Howard, N.I. Sokolov, J. Organomet. Chem. 637–639 (2001) 445.
[45] J. Lewis, P.R. Raithby, W.-Y. Wong, J. Organomet. Chem. 556 (1998) 219.
[46] W.-Y. Wong, H.-Y. Lam, S.-M. Lee, J. Organomet. Chem. 595 (2000) 70.
[47] W.-Y. Wong, W.-K. Wong, P.R. Raithby, J. Chem. Soc. Dalton Trans. (1998) 2761.
[48] W.-Y. Wong, K.-H. Choi, G.-L. Lu, Macromol. Rapid Commun. 22 (2001) 461.
[49] W.-Y. Wong, G.-L. Lu, K.-H. Choi, J.-X. Shi, Macromolecules 35 (2002) 3506.
[50] M.S. Khan, M.R.A. Al-Mandhary, M.K. Al-Suti, B. Ahrens, M.F. Mahon, L. Male, P.R. Raithby, C.E. Boothby, A. Köhler, Dalton Trans. (2003) 74.
[51] M.E. Wright, B.B. Cochran, Organometallics 12 (1993) 3873.
[52] P. Zanello, G. Opromolla, F.F. de Biani, A. Ceccanti, G. Giorgi, Inorg. Chim. Acta 255 (1997) 47.
[53] W.-Y. Wong, K.-H. Choi, G.-L. Lu, J.-X. Shi, P.-Y. Lai, S.-M. Chan, Organometallics 20 (2001) 5446.
[54] W.-Y. Wong, L. Liu, J.-X. Shi, Angew. Chem. Int. Ed. 42 (2003) 4064.
[55] S.J. Faville, W. Henderson, T.J. Mathieson, B.K. Nicholson, J. Organomet. Chem. 580 (1999) 363.
[56] P. Pyykkö, Chem. Rev. 97 (1997) 597.
[57] S.S. Batsanov, J. Chem. Soc. Dalton Trans. (1998) 1541.

[58] W.-Y. Wong, G.-L. Lu, L. Liu, J.-X. Shi, Z. Lin, Eur. J. Inorg. Chem. (2004) 2066.
[59] U.H.F. Bunz, Chem. Rev. 100 (2000) 1605.
[60] J.S. Wilson, A. Köhler, R.H. Friend, M.K. Al-Suti, M.R.A. Al-Mandhary, M.S. Khan, P.R. Raithby, J. Chem. Phys. 113 (2000) 7627.
[61] N. Chawdhury, A. Köhler, R.H. Friend, W.-Y. Wong, J. Lewis, M. Younus, P.R. Raithby, T.C. Corcoran, M.R.A. Al-Mandhary, M.S. Khan, J. Chem. Phys. 110 (1999) 4963.
[62] N. Chawdhury, A. Köhler, R.H. Friend, M. Younus, N.J. Long, P.R. Raithby, J. Lewis, Macromolecules 31 (1998) 722.
[63] J.S. Wilson, N. Chawdhury, M.R.A. Al-Mandhary, M. Younus, M.S. Khan, P.R. Raithby, A. Köhler, R.H. Friend, J. Am. Chem. Soc. 123 (2001) 9412.
[64] H.-Y. Chao, W. Lu, Y. Li, M.C.W. Chan, C.-M. Che, K.-K. Cheung, N. Zhu, J. Am. Chem. Soc. 124 (2002) 14696.
[65] W. Lu, H.-F. Xiang, N. Zhu, C.-M. Che, Organometallics 21 (2002) 2343.
[66] C.-M. Che, H.-Y. Chao, V.M. Miskowski, Y. Li, K.-K. Cheung, J. Am. Chem. Soc. 123 (2001) 4985.
[67] W.-Y. Wong, L. Liu, S.-Y. Poon, A.W.-M. Lee, K.-W. Cheah, J.-X. Shi, Macromolecules 37 (2004) 4496.
[68] C.S.-W. Lau, W.-T. Wong, J. Chem. Soc. Dalton Trans. (1999) 607.
[69] H. Schottenberger, K. Wurst, M.R. Buchmeiser, J. Organomet. Chem. 584 (1999) 301.
[70] K.R. Justin Thomas, J.T. Lin, Y.-Y. Lin, C. Tsai, S.-S. Sun, Organometallics 20 (2001) 2262.
[71] N.G. Pschirer, D.M. Ciurtin, M.D. Smith, U.H.F. Bunz, H.-C. zur Loye, Angew. Chem. Int. Ed. 41 (2002) 583.
[72] D.M. Ciurtin, N.G. Pschirer, M.D. Smith, U.H.F. Bunz, H.-C. zur Loye, Chem. Mater. 13 (2001) 2743.
[73] K.R. Justin Thomas, J.T. Lin, H.-M. Lin, C.-P. Chang, C.-H. Chuen, Organometallics 20 (2001) 557.
[74] P. Grosshans, A. Jouaiti, N. Kardouh, M.W. Hosseini, N. Kyritsakas, N. J. Chem. 27 (2003) 1806.
[75] C.J. Adams, J. Chem. Soc. Dalton Trans. (1999) 2059.
[76] B. Liu, W.-L. Yu, J. Pei, S.-Y. Liu, Y.-H. Lai, W. Huang, Macromolecules 34 (2001) 7932.
[77] M. Uekawa, Y. Miyamoto, H. Ikeda, K. Kaifu, T. Nakaya, Synth. Met. 91 (1997) 259.
[78] Q.D. Ling, E.T. Kang, K.G. Neoh, Macromolecules 36 (2003) 6995.
[79] X. Chen, J.-L. Liao, Y. Liang, M.O. Ahmed, H.-E. Tseng, S.-A. Chen, J. Am. Chem. Soc. 125 (2003) 636.
[80] J.C. Ostrowski, M.R. Robinson, A.J. Heeger, G.C. Bazan, Chem. Commun. (2002) 784.
[81] X. Gong, M.R. Robinson, J.C. Ostrowski, D. Moses, G.C. Bazan, A.J. Heeger, Adv. Mater. 14 (2002) 581.
[82] X. Gong, J.C. Ostrowski, D. Moses, G.C. Bazan, A.J. Heeger, Adv. Funct. Mater. 13 (2003) 439.
[83] X. Gong, J.C. Ostrowski, G.C. Bazan, D. Moses, A.J. Heeger, M.S. Liu, A.K.-Y. Jen, Adv. Mater. 15 (2003) 45.
[84] Y. Zhang, T. Wada, L. Wang, H. Sasabe, Chem. Mater. 9 (1997) 2798.
[85] S. Maruyama, X.T. Tao, H. Hokari, T. Noh, Y. Zhang, T. Wada, H. Sasabe, H. Suzuki, T. Watanabe, S. Miyata, J. Mater. Chem. 9 (1999) 893.
[86] K.R. Justin Thomas, J.T. Lin, Y.Y. Lin, C.W. Ko, J. Am. Chem. Soc. 123 (2001) 9404.
[87] Z. Zhu, J.S. Moore, J. Org. Chem. 65 (2000) 116.
[88] K. Brunner, A. van Dijken, H. Börner, J.J.A.M. Bastiaansen, N.M.M. Kiggen, B.M.W. Langeveld, J. Am. Chem. Soc. 126 (2004) 6035.
[89] P. Kundu, K.R. Justin Thomas, J.T. Lin, Y.-T. Tao, C.-H. Chien, Adv. Funct. Mater. 13 (2003) 445.
[90] Z. Zhu, J.S. Moore, J. Org. Chem. 65 (2000) 116.
[91] C.-H. Tao, K.M.-C. Wong, N. Zhu, V.W.-W. Yam, New J. Chem. 27 (2003) 150.
[92] G. Mosges, F. Hampel, M. Kaupp, P.V.R. Schleyer, J. Am. Chem. Soc. 114 (1992) 10880.
[93] P.N. Riley, P.E. Fanwick, I.P. Rothwell, Chem. Commun. (1997) 1109.
[94] P.N. Riley, R.D. Profilet, P.E. Fanwick, I.P. Rothwell, Organometallics 15 (1996) 5502.
[95] P.N. Riley, P.E. Fanwick, I.P. Rothwell, J. Chem. Soc. Dalton Trans. (2001) 181.
[96] P.N. Riley, R.D. Profilet, M.M. Salberg, P.E. Fanwick, I.P. Rothwell, Polyhedron 17 (1998) 773.
[97] R.D. Profilet, P.E. Fanwick, I.P. Rothwell, Polyhedron 11 (1992) 1559.
[98] D. Barr, A.J. Edwards, P.R. Raithby, M.-A. Rennie, K. Verhorvoort, J. Chem. Soc. Chem. Commun. (1994) 1627.
[99] G.B. Deacon, C.M. Forsyth, B.M. Gatehouse, P.A. White, Aust. J. Chem. 43 (1990) 795.
[100] W.J. Evans, G.W. Rabe, J.W. Ziller, Organometallics 13 (1994) 1641.
[101] C.T. Abrahams, G.B. Deacon, B.M. Gatehouse, G.N. Ward, Acta Cryst. C50 (1994) 504.
[102] M. Guan, Z.Q. Bian, F.Y. Li, H. Xin, C.H. Huang, New J. Chem. 27 (2003) 1731.
[103] V.C. Gibson, S.K. Spitzmesser, A.J.P. White, D.J. Williams, Dalton Trans. (2003) 2718.
[104] A.-C. Ribou, T. Wada, H. Sasabe, Inorg. Chim. Acta 288 (1999) 134.
[105] N.D. McClenaghan, R. Passalacqua, F. Loiseau, S. Campagna, B. Verheyde, A. Hameurlaine, W. Dehaen, J. Am. Chem. Soc. 125 (2003) 5356.
[106] F. Liu, K. Wang, G. Bai, Y. Zhang, L. Gao, Inorg. Chem. 43 (2004) 1799.
[107] A. Kimoto, J.-S. Cho, M. Higuchi, K. Yamamoto, Chem. Lett. 32 (2003) 674.
[108] L.J. Henderson Jr., F.R. Fronczek, W.R. Cherry, J. Am. Chem. Soc. 106 (1984) 5876.
[109] Y. Wang, W. Perez, G.Y. Zheng, D.P. Rillema, Inorg. Chem. 37 (1998) 2051.
[110] A.M. Pyle, J.P. Rehmann, R. Meshoyrer, C.V. Kumar, N.J. Turro, J.K. Barton, J. Am. Chem. Soc. 111 (1989) 3051.
[111] Y. Wang, W.J. Perez, G.Y. Zheng, D.P. Rillema, C.L. Huber, Inorg. Chem. 37 (1998) 2227.
[112] P. Kulkarni, S. Padhye, E. Sinn, C.E. Anson, A.K. Powell, Inorg. Chim. Acta 332 (2002) 167.
[113] P. Kulkarni, S. Padhye, E. Sinn, Inorg. Chim. Acta 321 (2001) 193.
[114] A.-P. Gu, R.-L. Zhang, G. Zhang, J.-S. Zhao, S.-Y. He, J.-M. Dou, D.-Q. Wang, Chin. J. Chem. 20 (2002) 1616.
[115] A. Baysal, J.A. Connor, J.D. Wallis, J. Coord. Chem. 53 (2001) 347.
[116] B.-L. Wu, H.-Y. Zhang, Q.-A. Wu, H.-W. Hou, Y. Zh, J. Mol. Struct. 655 (2003) 467.
[117] H.J. Eppley, S.M. Lato, A.D. Ellington, J.M. Zaleski, Chem. Commun. (1999) 2405.
[118] Z.-L. Lu, C.-Y. Duan, Y.-P. Tian, X.-Z. You, H.-K. Fun, B.-C. Yip, E. Hovestreydt, Polyhedron 16 (1997) 187.
[119] R.A. Klein, P. Witte, R.V. Belzen, J. Fraanje, K. Goubitz, M. Numan, H. Schenk, J.M. Ernsting, C.J. Elsevier, Eur. J. Inorg. Chem. (1998) 319.
[120] Q.-Y. Zhu, G.-Q. Bian, J. Dai, D.-X. Jia, J.-S. Zhang, L. Guo, Inorg. Chim. Acta 351 (2003) 177.
[121] W. Xiao, Z.-L. Lu, C.-Y. Su, K.-B. Yu, L.-R. Deng, H.-Q. Liu, B.-S. Kang, J. Mol. Struct. 553 (2000) 91.
[122] W. Xiao, Z.-L. Lu, X.-J. Wang, C.-Y. Su, K.-B. Yu, H.-Q. Liu, B.-S. Kang, Polyhedron 19 (2000) 1295.

[123] C. Xu, H.-Y. Mao, H.-Y. Zhang, Q.-A. Wu, H.-L. Liu, H.-W. Hou, Y. Zhu, G. Li, J. Mol. Struct. 658 (2000) 59.
[124] V.W.-W. Yam, Y. Yang, J. Zhang, B.W.-K. Chu, N. Zhu, Organometallics 20 (2001) 4911.
[125] V.W.-W. Yam, K.-Z. Wang, C.-R. Wang, Y. Yang, K.-K. Cheung, Organometallics 17 (1998) 2440.
[126] B.W.-K. Chu, V.W.-W. Yam, Inorg. Chem. 40 (2001) 3324.
[127] R.N. Warrener, A.B.B. Ferreira, A.C. Schultz, D.N. Butler, F.R. Keene, L.S. Kelso, Angew. Chem. Int. Ed. Engl. 35 (1996) 2485.
[128] M. Querol, H. Stoekli-Evans, P. Belser, Org. Lett. 4 (2002) 1067.
[129] F. Hintermaier, W. Beck, Polyhedron 17 (1998) 483.
[130] P.T. Witte, R. Klein, H. Kooijman, A.L. Spek, M. Polášek, V. Varga, K. Mach, J. Organomet. Chem. 519 (1996) 195.